National Oceanography Centre

Application of X-band radars for deriving intertidal bathymetries and characterising coastal behaviours

Lyddon, C.E.[1], Bird, C.[2], Brown, J.M.[3], Plater, A.J.[1]

[1] Department of Geography and Planning, University of Liverpool, L69 7ZT, UK

[2] Marlan Maritime Technologies Ltd, Liverpool, UK

[3] National Oceanography Centre, Liverpool, L3 5DA, UK

2021

Internal document number 23

Abstract

Coastal monitoring techniques aim to capture the relationship between physical forcing factors and morphological change, at a range of timescales to understand ongoing coastal processes and identify areas prone to erosion and flooding hazards posed by storms. Standard marine radar provides temporally and spatially continuous monitoring data over a wide area in all conditions, and images can be processed to generate intertidal bathymetries to assess morphological change across event (days-years) timescales. This research applies a series of intertidal bathymetries derived from a standard marine radar deployed at Camber Sands, southeast England in XBeach, a process-based, storm response model, to assess wave runup hazard at the coast during a high energy storm event from the deployment period. Wave runup is dependent on offshore wave climate and beach slope and used here as a proxy to explore the influence of nearshore morphological variability, represented by different processing techniques to derive intertidal bathymetries from the marine radar images, on a coastal hazard. XBeach is used in combination with beach survey data from the site to first demonstrate reasonable skill in reproducing wave runup observations. Intertidal bathymetries are derived from the marine radar images using either a local or regional water level signal, and an average of 1, 5, or 10 days of images preceding the storm event. Modelled wave runup shows up to 0.32 m sensitivity to input intertidal bathymetries, which could be important for overwash predictions. The slope and resolution of the radar-derived intertidal bathymetries is sensitive to the water level time series used. This research is the first time that radar-derived intertidal bathymetries have been used to assess a coastal hazard in a process-based model, and results show that ideally users would have a locally measured water level to accurately generate intertidal bathymetries, and extended beach surveys for ground truthing.

Abbreviations for different DEMs are explained in the text and placed here as a reference:

Digital Elevation Model	**Abbreviation**
CS_DEM from interpolated LiDAR	CS_DEM
Camber Sands idealised slope from interpolated LiDAR	CS_IS
X-band radar-derived DEM processed from local Met Office North West European Shelf seas modelled water level outputs	XBR_DEM_NWS
X-band radar-derived idealised slope processed from Met Office North West European Shelf seas modelled water level outputs	XBR_IS_NWS
X-band radar-derived DEM processed from regional Dover tide gauge observation water level	XBR_DEM_DOV
X-band radar-derived idealised slope processed from regional Dover tide gauge observation water level	XBR_IS_DOV

1. Introduction

Coastal morphology is known to respond to physical forcing factors on a range of time scales, from short-term storm response (Didier *et al.*, 2020; Barnard *et al.*, 2014), to long-term seasonal and annual changes due to natural and anthropogenic influences (Biausque and Senechal, 2018; Splinter *et al.*, 2017). Strategic coastal monitoring aims to capture coastal behaviours, such as the relationship between morphological change and hydrodynamics, and understand ongoing coastal processes to inform shoreline management plans and hazard assessments (Parsons *et al.*, 2016; Kerguillec *et al.*, 2019). Long-term monitoring strategies can help to inform shoreline management plans over three management epochs (present day: 0-20 years; medium-term: 20-50 years; long-term: 50-100 years) (Brown et al., 2016) and identify how the coast can respond and adapt to climate change (Burningham and French, 2017). However, morphological change also needs to be captured and resolved at a shorter time scale; instantaneous processes, such as a change in a wave period, direction or height, can alter a beachface or bedforms over seconds to days (Cowell and Thom, 1994). An understanding of the impact of higher frequency, short-term storms events on coastal morphology and behaviours is required, but not currently considered, in management plans to help to inform predictions of present and future coastal hazards (Williams *et al.*, 2015).

High energy storms generated by low atmospheric pressure systems and hurricanes can elevate water levels and generate increased wave action at the coast, which can act as a key driver of morphological change and backshore flooding (Cohn and Ruggiero, 2016; Pollard *et al.*, 2018). Wave action is a strong control on beach morphology (Phillips *et al.*, 2017; Burvingt *et al.*, 2017), and can cause short-term (episodic) erosion which threatens ecological integrity and coastal infrastructure (Vousdoukas *et al.*, 2011). Storm-induced changes in beach morphology may only recover if local sediment supply is sufficient (Ferreira et al., 2017). Waves also pose a hazard in themselves at the coast, and water level at the shoreline during storm events can be substantially increased by wave runup, which is the maximum vertical extent of wave uprush on a beach following wave breaking (Stockdon *et al.*, 2006, 2014), surface and infragravity waves (Senechal *et al.*, 2011). The onshore extent of wave runup is dependent on the offshore wave climate and variability of beach morphology and foreshore slope, making it a highly site-specific parameter (Serafin *et al.*, 2017). A steeper foreshore slope, such as those seen on gravel barriers and pebble beaches (Poate *et al.*, 2016), will generate a larger wave runup than on shallow sandy beaches or those which are fetch limited (Palmer *et al.*, 2014). Wave runup can be used as an indicator of how beach morphology and beach slope influence the processes associated with a storm induced hazard, and a proxy for potential overwash and flooding hazards (Didier *et al.*, 2020). Assessment of local coastal behaviours, including beach erosion and wave runup, over storm event timescales can identify areas prone or resistant to erosion and wave runup hazards (Ciavola *et al.*, 2014).

Techniques for monitoring coastal behaviours

The assessment of local coastal behaviours should aim to accurately capture and quantify changes in shoreline position and foreshore slope over space and time with high quality, continuous datasets (Bradbury *et al.*, 2003). Regular, long-term coastal monitoring programmes which collect records of beach elevation changes along cross-shore profiles provide insights into morphodynamic behaviours which cannot be achieved from infrequent, event-led measurements (Turner *et al.*, 2016). These traditional methods rely on repeated sampling of erosion and accretion, observations of bedforms, and recording wave and water level conditions over time (Pye and Smith, 1988) but are labour intensive and require resource commitment over the longer term to be useful. Other options for collecting local scale beach morphology data include Unmanned Aerial Vehicles (UAV), which have been used to capture the dynamic behaviour of beach cusp systems in response to local

hydrodynamics (Nuyts *et al.*, 2020). Fixed, time-lapse cameras and video monitoring systems have also been used to monitor beach state, dune settings and wave climate during high-energy storm events (Davidson *et al.*, 2006; Oh *et al.*, 2020; Guisado-Pintado and Jackson, 2020). Airborne and terrestrial topographic Light Detection and Ranging (LiDAR) surveys capture shoreline position and beach profiles over wider spatial scales (Hobbs *et al.*, 2010; Klemas, 2011) but require large financial investments and are temporally infrequent. Standard marine navigation radar, operating at X-band frequency, and nearshore remote sensing infrastructure can continuously and remote collect morphological and hydrodynamic data in all weather conditions (Bell *et al.*, 2016). These technologies have been used to robustly map intertidal zone elevations over large spatial scales (up to 5 km) at a reduced cost. These surveys can quantify and characterise morphological response to high-energy storm events by comparing pre- and post-storm surveys and can be used in combination to capture site-specific behaviours (Wallbridge *et al.*, 2019).

X-band radar-derived intertidal morphologies

Shore-based, marine navigational radar operating at X-band frequency is increasingly used to map and monitor intertidal morphological change (Bell *et al.*, 2016; Bird *et al.*, 2017). X-band radars can be deployed as a cost-effective means to observe short- and long-term changes in nearshore bathymetry-topography at improved temporal and spatial resolution (Bell *et al.*, 2016; Atkinson *et al.*, 2018) and can complement other survey techniques by filling gaps in pre- and post-storm morphology data (Williams *et al.*, 2015; Parsons *et al.*, 2016). A temporal radar waterline method has been developed to generate intertidal morphologies and digital elevation models (DEMs) to captures details of coastal behaviours by identifying the elevation of wetting and drying transitions in each radar image over time (Bell *et al.*, 2016). Pixel intensity in a radar image over a set period is used to indicate episodic tidal cycles of wetting and drying. The method requires an accurate, local water level time series to represent the tidal range near the radar deployment. The water level time series is used as an altimeter to determine if a pixel within the radar image should or should not be covered by the tide at the corresponding time (Wallbridge *et al.*, 2019). An accurate X-band radar-derived intertidal morphology and DEM is also dependent on the radar capturing sufficient signal from the sea surface, so deployment in tidal areas exposed to high energy conditions is preferable. An increase in surface water roughness, directly caused by underlying topographic and bathymetric variation, will also improve the quality of radar image. X-band radar-derived intertidal morphologies and DEMs have been successfully used to monitor morphological evolution in the intertidal zone at in the Dee Estuary, northwest England over a two-week tidal cycle (Bird *et al.*, 2017) and several years of change (Wallbridge *et al.*, 2019). Multiple one- and two-dimensional cross-shore beach profiles can be extracted from the X-band derived DEMs to analyse their evolution over time and observe changes in bedforms. As already explained, high-energy storm events not only influence variability in beach morphology and foreshore slope, but also wave conditions. Therefore this research aims to explore the application of X-band radar-derived intertidal morphologies for deriving storm-induced wave runups as an indicator of how beach morphology influences the processes associated with a storm-induced hazard.

Characterising coastal behaviours through application of radar-derived bathymetries

Process-based, shoreline response models can be used to reproduce the processes occurring in coastal areas during high-energy storm events, including wave runup, overwash, infragravity waves, and erosion (Roelvink *et al.*, 2009). Numerical models, such as XBeach (Roelvink *et al.*, 2009) can be used to simulate coastal morphodynamics, e.g. (Vousdoukas *et al.*, 2011) for sand and (McCall *et al.*, 2015) on gravel beaches, and to explore the effect of cross-shore and alongshore processes acting on the coastal environment. XBeach has been successfully used to simulate erosion and wave runup

hazards on sandy coastlines worldwide (McCall *et al.*, 2010; Phillips *et al.*, 2017). Regardless of whether the model is used in one-dimensional or two-dimensional mode, all models require a series of data inputs, including coastal topography-bathymetry over which physical processes occur. X-band radar-derived intertidal morphologies can be used as input depth files in process-based numerical models. Wave runup can be simulated using these models as an indicator of the influence of nearshore morphological variability on coastal behaviours (Ferreira *et al.*, 2017)

X-band radar-derived intertidal morphologies are only as accurate as the water level time series used in the temporal waterline algorithm. An onsite tide gauge, deployed as part of an ongoing coastal monitoring programme or at the same time as the X-band radar deployment, would provide the most accurate water level record. However this is not a local control available to all coastal monitoring programmes, due to cost and equipment availability. Water level records are available from alternative sources within the UK, including national tide gauges from the British Oceanographic Data Centre and global ocean models, such as the Met Office North West European Shelf seas model which is available at 1.5 km resolution (Siddorn *et al.*, 2015; Saulter *et al.*, 2016) . The resolution and coverage of X-band radar-derived intertidal morphologies is also dependent on the period used to calculate the mean elevation of the radar-observed waterline, which is defined by the user but has been shown to produce accurate results when averaged over a 5 to 10 day window (Bird *et al.*, 2017).

This research aims to explore the application of X-band radars for deriving the intertidal bathymetries and wave runups where you do not have local reference level from a tide gauge. The effect of different water level records and processing techniques on the temporal waterline algorithm is quantified by applying a series of X-band radar-derived morphologies in XBeach to simulate wave runup at Camber Sands, southeast England. Wave runup is used as an indicator to demonstrate the influence of nearshore morphological variability on local coastal behaviours and hazards. To the authors' knowledge, this is the first time that;

- 2D profiles have been extracted from a radar-derived DEM to align with established, industry-standard methods for monitoring coastal morphological change.
- The potential to derive radar-derived DEMs from regional modelled tidal levels where local tide gauge control is absent is examined.
- Exploring the efficacy of using radar-derived DEMs (and extracted 2D profiles) for assessing: a. wave runup hazard (and changes therein) and b. morphological change over instantaneous timescales determined by the following phenomena: i. high tidal level, ii. high wave height, iii. high wave hazard, is examined.
- The duration of radar data required to capture changes in coastal morphology is assessed.

In section 2 we first demonstrate that XBeach skillfully reproduces wave runup by simulating low and high energy conditions at Camber Sands, southeast England when beach survey data is available. Section 2 then explains how outputs from the X-band radar data are processed and applied in XBeach. Section 3 presents results from XBeach including i) wave runup time series; ii) maximum wave runup at time of high water; and iii) area under curve of the time series to show the influence of nearshore morphological variability from the series of X-band radar-derived intertidal morphologies on wave runup. Section 4 discusses how best to apply X-band radar-derived intertidal morphologies to characterise local coastal behaviours, best practices, and suggestions for future work.

1.1. Case study

The study site is Camber Sands, southeast England (Figure 1), which lies within the Dungeness, Romney Marsh and Rye Bay Site of Special Scientific Interest (SSSI).

Camber Sands is described as a broad and dissipative low-energy, fetch-limited sand beach with a low-amplitude, shallow sloping sandy terrace (Billson *et al.*, 2019). The gently shelving, low tide terrace beach is dominated by extensive ridge and runnel morphology. The largest natural sand dune system in Sussex is located to the west of Camber Sands and is backed by a golf course. The beach towards the east of Camber Sands forms a composite sand and gravel beach and is more heavily managed with re-nourished gravel and rock armour backed by a seawall, including the Broomhill Sands Coastal Defence scheme (Environment Agency, 2014). Further east is Dungeness, a large cuspate foreland composed and gravel barrier system.

The macrotidal location has a mean high-water spring tide of 3.54 m OD (ordnance datum). The December 6 2013 storm generated a 1.63 m skew surge at the nearest tide gauge at Dover, and a 1 in 843 year return period (SurgeWatch, 2020). The location experiences a bimodal, bidirectional wave climate. The closest wave buoy, Hastings WaveNet at 50°44'.79N, 000°45'.29E, shows that the largest waves approach from the southwest with a significant wave height up to 5 m and a peak period up to 18 seconds (Mason *et al.*, 2009). The dominant wave direction is from the southwest due to the orientation of the shoreline.

Camber Sands is of a high value in terms of protected habitat and is an important location for geomorphology, plant and invertebrate communities, as well as a site for a wide range of recreational uses and critical energy infrastructure. Annual beach surveys available from Canterbury Council and the Channel Coastal Observatory, as well as high resolution LiDAR surveys, in addition to storm surveys and standard marine X-band radar deployment, make this a suitable location to assess how best to use monitoring and models for characterising coastal behaviours.

2. Methods

The research applies the process-based, morphological model XBeach to Camber Sands for the same period that storm surveys collected from 19 to 22 November 2016, by the University of Plymouth Coastal Marine Applied Research (CMAR) group, and outputs from an X-band radar deployed by Marlan Maritime Ltd from 16 November 2018 – 30 June 2019. The monitoring data are available for two separate periods, and so two stages of modelling are presented here.

2.1. XBeach

The process-based, storm impact model XBeach (October 2015 “Kingsday” version, Roelvink et al., 2009) is applied to Camber Sands to study the effect of a single storm on wave runup hazard and beach morphology (short-term influence). XBeach operates over a depth file to represent local bathymetry, and solves coupled 2D horizontal equations for wave propagation, flow, and sediment transport based on offshore wave and tidal boundary conditions over the course of a model simulation (Wallbridge *et al.*, 2019). XBeach can operate in non-hydrostatic mode where all waves are resolved, or hydrostatic mode where short wave amplitude variation is solved separately from the long waves, currents and morphological change. The model conserves mass and is specifically designed to model beach erosion during storms; it is the most common model applied to simulate the impact of storm events on sand beaches (Parsons *et al.*, 2016). The model must be tuned and calibrated to accurately represent morphological change and wave runup at a beach location using a series of switches e.g. to enable morphological development, sediment transport processes, and wave-current interaction. As the beach at Camber Sands is composed of sand and a fixed sea wall, XBeach is a suitable model to use for this study.

These sections describe the methods and data used to set up the transects and the boundary conditions to force XBeach, which is applied here in hydrostatic mode as a 1D cross-shore profile model, for model calibration and then to assess wave runup hazard.

2.2. Model calibration

2.2.1. Digital Elevation Model from LiDAR

A 2D Digital Elevation Model (DEM) was developed for Camber Sands (CS), southeast England, from which a series of 1D cross-shore profiles were extracted and used as depth files in XBeach. The 2D CS_DEM was created using a combination of offshore, 1 arcsecond bathymetry (cell size approximately 30 m) (Edina Digimap, 2020), 25 cm composite LiDAR data at the upper beach and behind the seawall, which was a raster dataset made up of the most accurate DEMs collected over time (Edina Digimap, 2020), and 1 m LiDAR from the Channel Coastal Observatory, collected as part of the South East Coastal LIDAR Programme in October 2018, in the intertidal zone (Channel Coastal Observatory, 2020). The data were interpolated and combined in ArcMap resampled to 1 metre, and the DEM is 8.6 km x 9 km (see Figure 1). The CS_DEM shown in Figure 1 is used as a baseline to represent a standard modelling approach that uses available observations from national monitoring programmes for this the study.

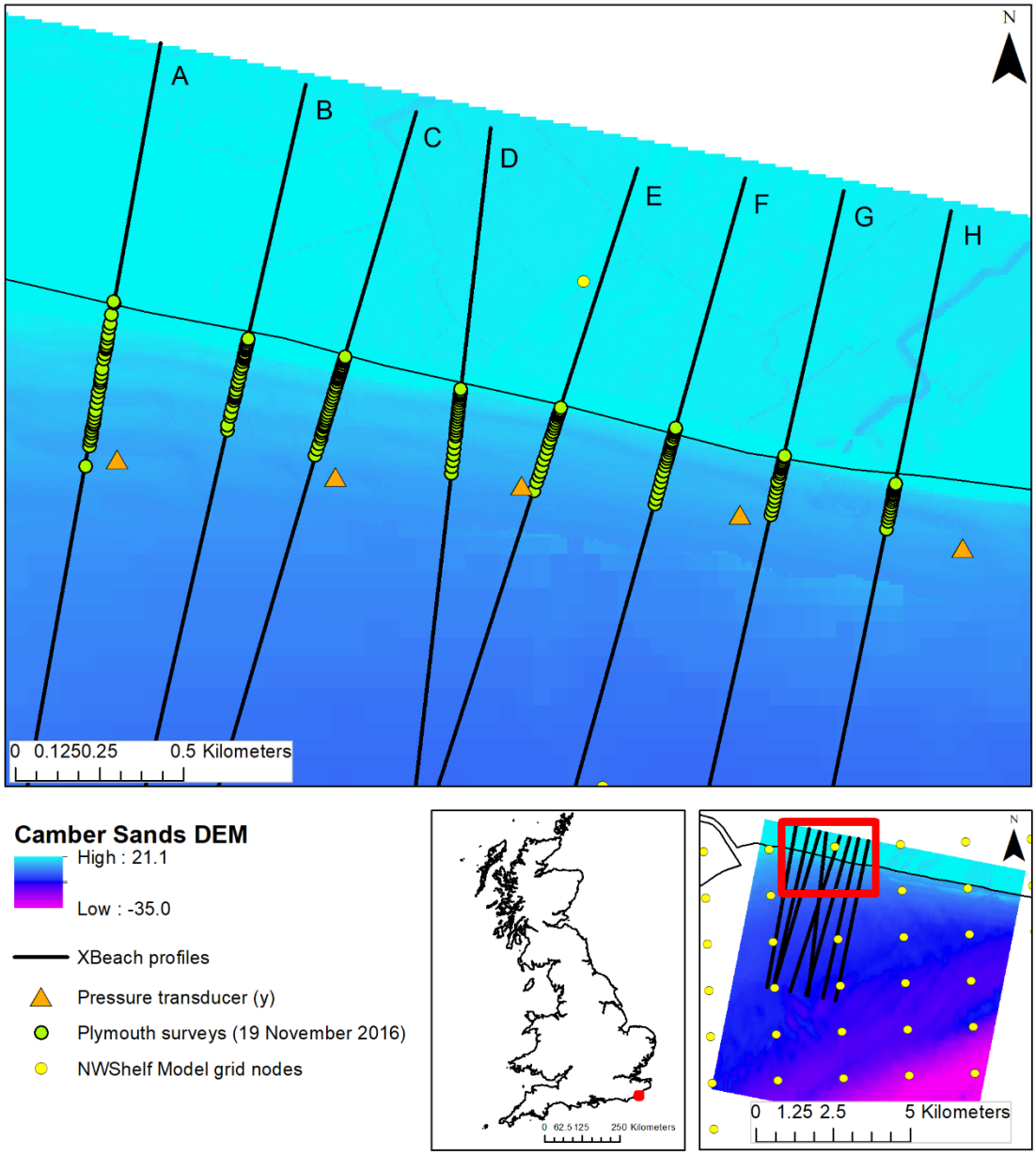

Figure 1: CS_DEM (offshore bathymetry; composite LiDAR; intertidal LiDAR) including the location of eight cross-shore Plymouth beach morphology surveys (green dots); five alongshore pressure transducers (orange triangle); eight cross-shore XBeach profiles extended offshore; UK Met Office North West European Shelf seas model grid nodes (yellow dots).

2.2.2. Cross-shore beach profiles for model calibration

Storm surveys were completed at Camber Sands from 19 to 22 November 2016 by the University of Plymouth Coastal Marine Applied Research (CMAR) group. Morphological change over the storm survey period was recorded by completing beach morphology surveys along eight cross-shore profile lines during each daylight low tide. The beach morphology surveys extend from the top of the beach (where sea defences end) to the low water position, using RTK GPS (x and y is provided in British National Grid coordinate system and z is relative to Ordnance Datum). The profile lines were pre-defined and contribute to a long-term regional monitoring program undertaken by the local

authority. Five RBR Solo D-Wave Pressure transducers were deployed along-shore at bed level and logging continuously at 8Hz to record wave behaviour over the storm event. As seen in Figure 1, the location and angle of the eight beach morphology surveys, lettered A-G, are used to determine the location of the 1D cross-shore profiles to be used in XBeach. The Plymouth beach surveys were extended up to 4.2 km offshore to determine the sub-tidal profile gradient and the offshore limit represents the location at which the offshore boundary conditions were applied from the Met Office North West European Shelf seas model (Wallbridge *et al.*, 2019), a 1.5 km operational model based on the NEMO ocean model, at grid nodes lat/long *50.9054, 0.7878* and *50.9054, 0.8181*. Elevation data was extracted along the length of these profiles, 5.5 km, from the CS_DEM at a resolution of 15 m, and provided eight baseline surveys.

Beach morphology surveys were collected everyday over a 4-day period from 19 – 22 November, so 4 different beach morphology surveys were available for each profile. The elevation data for each daily beach morphology survey was embedded into these extended baseline profiles from the CS_DEM, shown as green dots in Figure 1, to provide a time-series of morphological change along each profile. The eight cross-shore 1D profiles with elevation data from just the CS_DEM, and profiles with the Plymouth beach morphology survey data embedded in, are processed in Matlab to generate a series of .dep files as input for XBeach.

2.2.3. Model calibration scenarios

Eight baseline profiles from the CS_DEM and eight profiles which included the Plymouth beach morphology surveys were used in XBeach in hydrostatic mode in a series of scenarios to test the model's ability to simulate morphological evolution and wave runup.

The scenarios were designed to test how well XBeach can develop and evolve the beach morphology along each cross-shore profile from one survey to the next. Table 1 provides detail of the timing of the four periods simulated. Figure 2a shows the four Plymouth beach morphology surveys and the Camber Sands baseline DEM along profile D as an example selected on the basis that it is located between two pressure transducers and is, therefore, assumed to represent beach dynamics due to its central location among the other surveys. Figure 2b shows the intertidal zone. Scenario 1 aims to test if XBeach could evolve the Plymouth beach morphology survey from 19 November 2016, embedded in the CS_DEM, to reflect the survey on 20 November 2016. All scenarios were tested with morphological evolution and sediment transport enabled (1) or disabled (0) in XBeach. XBeach bed level (zb) outputs were compared to the Plymouth profile after the subsequent high water to determine if the model can evolve morphology from the first to the second profile. Bed level (zb) was output from the model every 15 minutes over the duration of the model simulation to determine the model's ability to evolve morphology.

Table 1: Scenarios run for model calibration

Model run	Dates	Conditions
1	19-20 November	1 day
2	21-22 November	1 day
3	19-22 November	4 days: survey duration
4	21-22 November	1 day fixed intertidal zone to stop morphology evolving in that section: evolves in swash zone only

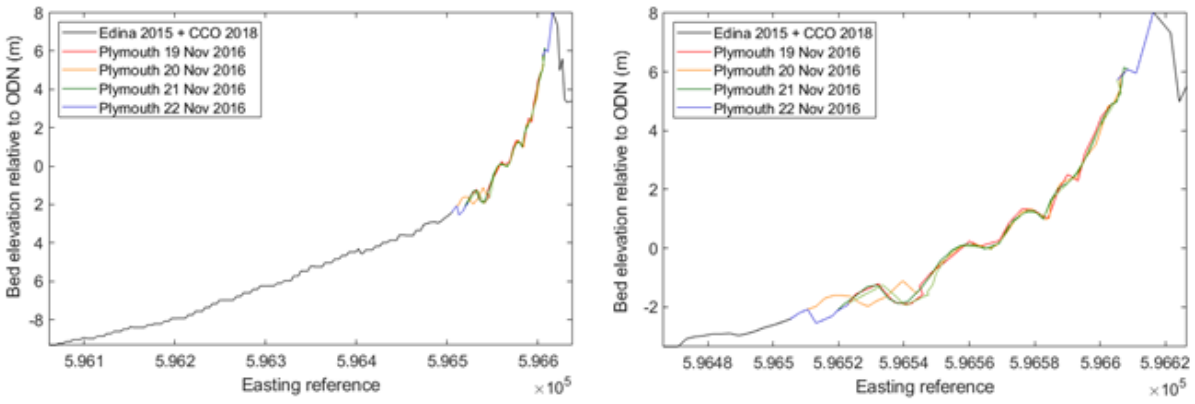

Figure 2: Change in intertidal bathymetry along Profile D for each Plymouth beach morphology survey embedded in the Edina baseline data.

A wave runup gauge ("nrugauge = 1") was set in the model to calculate wave runup in the swash zone. Wave runup from each profile ("point_zs") was compared to the observed wave runup recorded by the pressure transducers for each simulation, to determine the sensitivity of runup hazard to beach morphology and model setup (i.e. morphological development switches on or off). A correlation coefficient (R^2) was calculated to assess the ability of the model to simulate wave runup.

All simulations were tested with sediment transport and morphological evolution switched on and off in XBeach to explore the sensitivity of the model and outputs to these parameters ("morphology = 0/1"; "sedtrans = 0/1"). Scenario 4 utilises the "ne_layer" keyword in the parameter file to fix offshore morphologies and control the movement of sediment along the profile. Each grid point in the transect is assigned a value from zero for non-erodible at the offshore grid points, or 10 for erodible in the intertidal zone. The typical simulation time was 30 minutes, with a time step of 0.02 s, which is sufficiently small to capture wave runup conditions.

2.2.4. Boundary conditions

Outputs from the UK Met Office North West European Shelf seas model were used as boundary conditions throughout this study. The 1.5 km resolution ocean model, based on NEMO, is forced by the UK Met Office North Atlantic Ocean forecast model, and provides hourly water level relative to the geoid. The model outputs account for surge, atmospheric pressure, wave current interaction, and shallow water processes (Saulter et al., 2016; Siddorn et al., 2016) WAVEWATCH III is forced the UK Met Office Global wave forecast model, atmospheric forcing is provided by the operational ECMWF Numerical Weather Prediction model, and surface current forcing is provided by the North-West Shelf ocean physics analysis and forecast. Outputs from WAVEWATCH III include hourly significant wave height, peak period, wave direction, and directional spreading.

Boundary conditions for the calibration study were provided directly from the UK Met Office. Data was provided in netCDF format, which was processed in Matlab to generate boundary conditions for the period of the storm surveys (see Figure 3). An hourly water level time series (tide + surge) was used to force the offshore boundary of each profile for the duration of the scenario (*zs0file = tide.txt; tideloc = 1*). The wave characteristic time series from WAVEWATCH III were used to create a JONSWAP spectra, with the jonstable switch (*instat = 4; bcfile = bcfile.txt*), providing wave height, peak period, direction, spreading every hour at the offshore boundary (see Table 2). JONSWAP refers to Joint North Sea Wave Project, an empirical relationship for a wave spectrum that defines the

distribution of the wave energy frequency (Hasselmann et al., 1973), and models the propagation and decay of a set of waves. Wind was not accounted for in this study. An average value was calculated and applied for directional spreading based on 5 years wave data from the Met Office North West European Shelf seas model outputs.

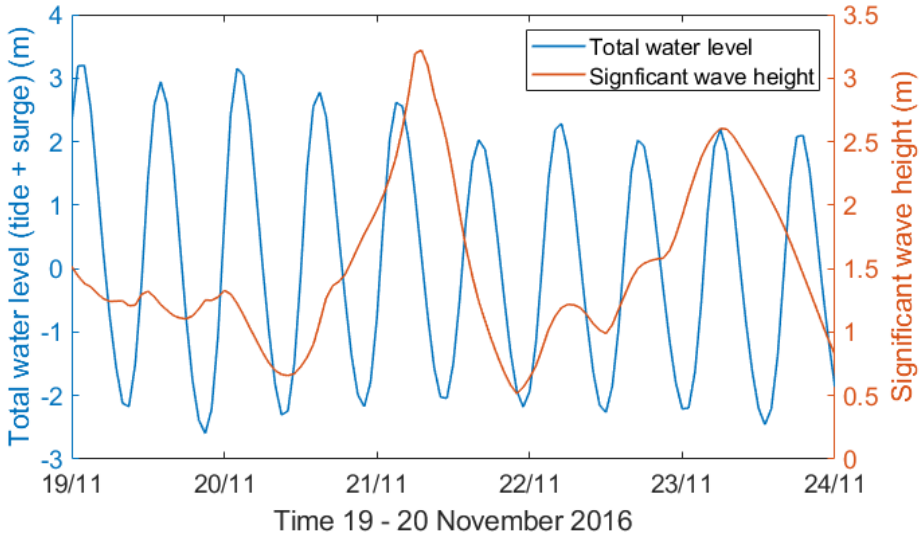

Figure 3: Water level and wave time series from the UK Met Office North West European Shelf seas model (NEMO and WAVEWATCH III) for the 4 day simulation from grid node *50.9054, 0.7878* for the duration of the survey period (19-22 November 2016).

Table 2: Example JONSWAP (jons_1.txt) XBeach input

Hm0 = 0.766
Tp = 4.26
mainang = 226.1
gammajsp = 3.3
s = 21
Fnyq = 0.3

2.2.5. Survey results

Morphological evolution and wave runup results from profile B, D, and G are presented in the following section as representative of all results.

2.2.5.1. Morphological evolution

Four scenarios are run to explore the ability of XBeach to develop and evolve the intertidal morphology over different dates and conditions during the period of Plymouth beach surveys. These scenarios aim to determine the models ability to simulate morphological evolution by testing to see if the input survey (which is embedded in the baseline LiDAR profile) develops to replicate the survey data recorded on the following day or later in the week. Bed level outputs from XBeach scenarios which are run with morphological development and sediment transport switches turned off are identical to the bed level inputs (there is no evolution), so these results are not included in this section.

The results from profile D are presented here as representative of results for all profiles. The profile with Plymouth beach morphology survey data from 19 November 2016 embedded into the CS_DEM is shown in Figure 4 (solid black line) and is used as the input in scenario 1. The bed level at the end of the 1 day simulation for scenario 1, on 20 November 2016, to show how the XBeach evolves the profile with morphological development and sediment transport turned is shown in blue. The Plymouth beach survey from 20 November 2016 is shown in Figure 4 in purple. In respect to Figure 4, the analysis aims to determine if the input profile (black line) develops into the output profile (blue line), so that it resembles the next survey (purple line). XBeach has developed the morphology so that there is a change from the input to output profile, and the ridge and runnel system along the profile remain largely in the same place in the output profile (blue line). The model appears to smooth the profile, and infill some of the troughs, notably at easting reference 596566 and 596585. It can be seen from Figure 3 that 19 – 20 November 2016 were low energy conditions and as a storm response model, XBeach may not show much change during this period.

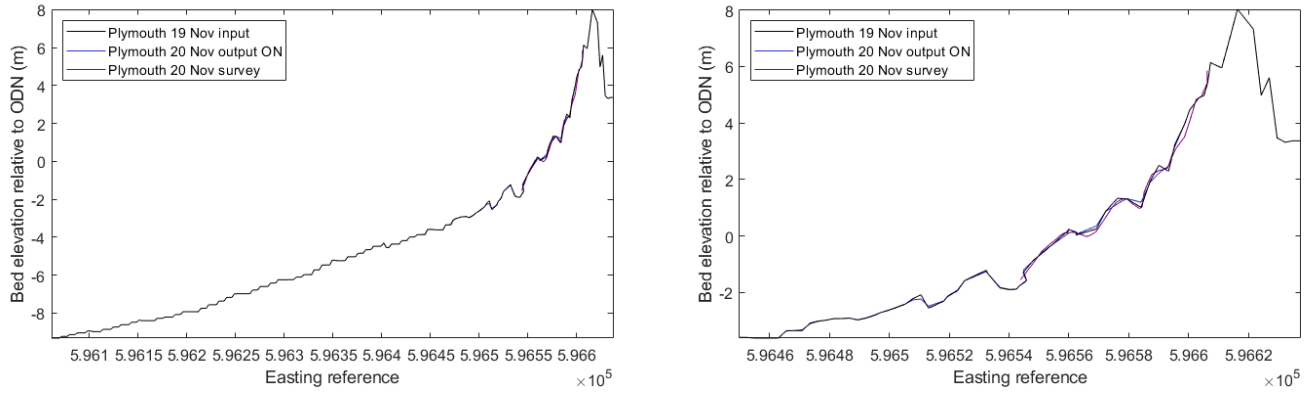

Figure 4: XBeach input and output profiles for 19-20 November 2016 scenarios under low energy conditions including i) the CS_DEM with 19 November beach morphology survey embedded (black line); ii) XBeach output on 20 November with morphological development and sediment transport ON (blue line); and iii) 20 November beach morphology survey (purple line).

XBeach was run over a higher energy period in scenario 2, from 20 – 21 November 2016. The profile with Plymouth beach morphology survey data from 20 November 2016 embedded into the CS_DEM is shown in Figure 5 (solid black line) and is used as the input in scenario 2. The bed level at the end of the 1 day simulation for scenario 2, on 21 November 2016, to show how the XBeach evolves the profile with morphological development and sediment transport turned is shown in blue. The Plymouth survey from 21 November is shown in purple. This period represents more active hydrodynamic forcing, as the waves are larger. The definition in the ridge runnel system is lost; XBeach smooths the profile over the duration of the scenario (shown by the solid blue line), and not only infills the lows but also smooths out the highs. The Plymouth beach survey on 21 November 2016 identifies the offshore movement of a ridge at easting reference 596530, but this is not replicated in the XBeach scenario.

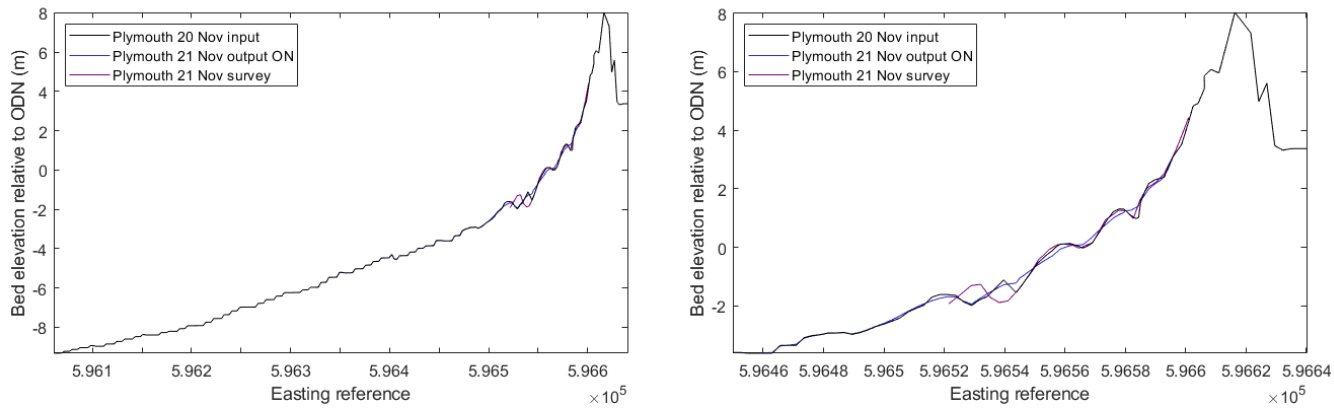

Figure 5: XBeach input and output profiles for 20-21 November 2016 scenarios under higher energy conditions including i) the CS_DEM with 20 November beach morphology survey embedded (black line); ii) XBeach output on 21 November with morphological development and sediment transport ON (blue line); and iii) 21 November beach morphology survey (purple line).

XBeach was run over the duration of the Plymouth beach surveys in scenario 3 from 19 – 22 November 2016. The profile with Plymouth survey data from the 19 November 2016 embedded into the CS_DEM is shown in black in Figure 6. The bed level at the end of the 4 day simulation, on 22 November 2016, is shown in blue, in addition to the Plymouth beach morphology survey from 22 November 2016. XBeach replicates the elevation of the peak of the ridge offshore between easting reference 596520 and 596540 and the trough between 596540 and 596545, compared to the survey on 22 November 2016. However, XBeach smooths the overall appearance of the beach ridges across profile by reducing the highs and infilling the lows.

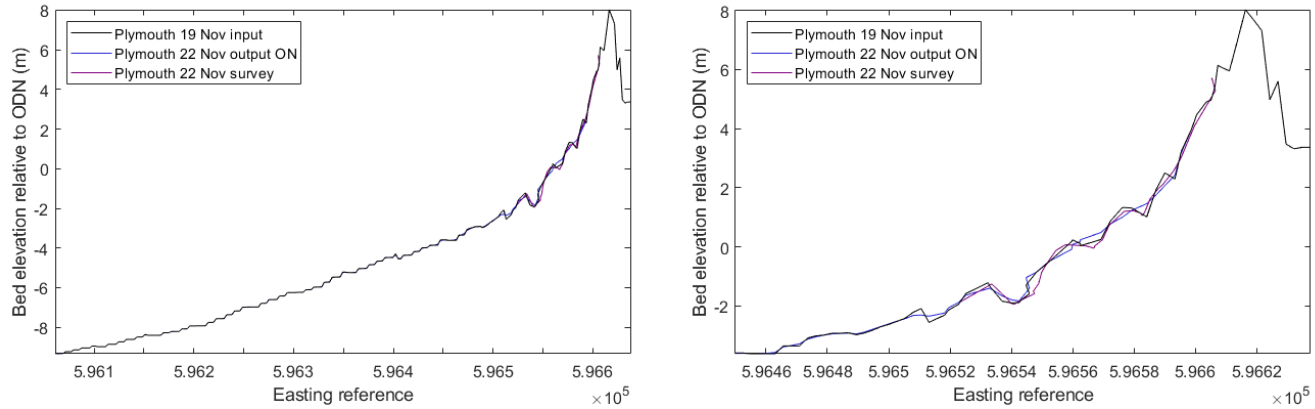

Figure 6: XBeach input and output profiles for 19-22 November 2016 scenarios for duration of survey including i) the CS_DEM with 19 November beach morphology survey embedded (black line); ii) XBeach output on 22 November with morphological development and sediment transport ON (blue line); and iii) 22 November beach morphology survey (purple line).

XBeach is run for the higher energy, 1 day scenario again (20 – 21 November 2016), with the intertidal morphology fixed using the "ne_layer" keyword in the parameter file. This scenario fixes the offshore morphology up to the point where the Plymouth beach morphology survey begins, to determine if this switch stops the intertidal zone being smoothed. Figure 7 shows the input profile with Plymouth survey data from the 20 November 2016 embedded into the CS_DEM in black, and the output bed level from 21 November 2016 for scenario 2 in blue and scenario 4 with the fixed intertidal morphology in green. The Plymouth beach morphology survey from 21 November 2016 is

shown in purple. The output bed levels from XBeach, in blue and green, are very similar and there is a small impact on evolution of morphology when the intertidal section is fixed. The trough at easting reference 596582 is still infilled, but 0.07 m shallower than scenario 2 when the intertidal morphology is not fixed. The difference between scenario 2 and 4 does not exceed 0.07 m.

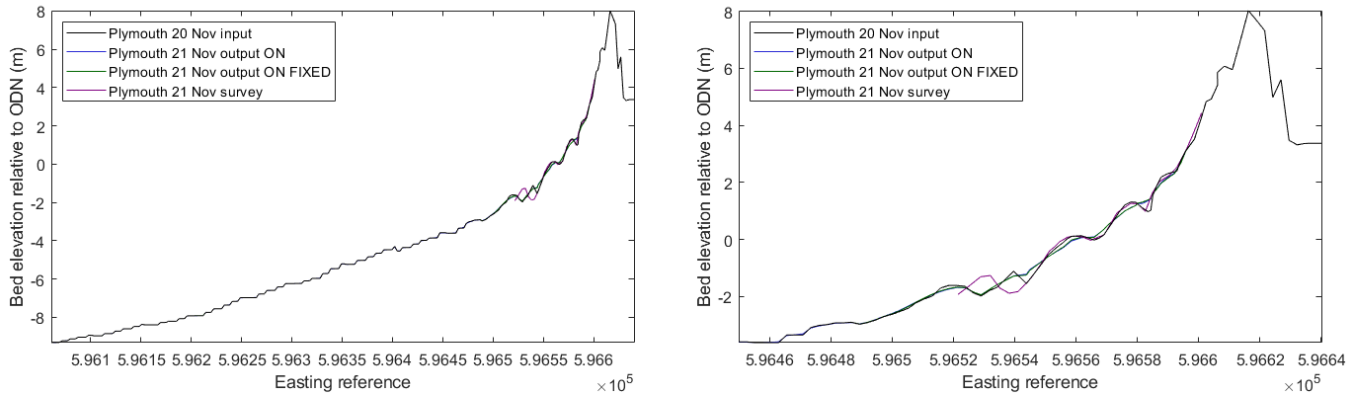

Figure 7: XBeach input and output profiles for 20-21 November 2016 scenarios under higher energy conditions with a fixed intertidal zone including i) the CS_DEM with 20 November beach morphology survey embedded (black line); ii) XBeach output on 21 November with morphological development and sediment transport ON (blue line); and iii) 21 November beach morphology survey (purple line).

These calibration scenarios show that XBeach largely smooths the morphology of upper sections of the profile over the duration of each scenario, but it able to maintain the overall slope of the profile and the position and altitude of some crests further offshore. This is most notably over the 4 day simulation. XBeach is a storm response model and these results show that it is best used over the period of a storm event (e.g. 12 hours). Inaccuracies in the elevation of the ridge runnel systems in the model outputs may be due to errors in shallow water bathymetry which alters wave propagation. Further to this, the profiles are 2DH and there is no account for alongshore sediment transport, which may contribute to the evolution of the morphology during storm events.

2.2.5.2. Net losses and gains along the profile

It has been shown that XBeach is able to maintain the overall beach slope in the intertidal zone, but also smooths the profile so detail in the ridge runnel system is lost. The following section explores whether XBeach can maintain sediment volumes along profile D, even if it loses the definition of the intertidal morphology. This section considers the volumetric changes in the profiles, represented by change in area under the curve (trapezoid method) and compares the percentage change in area under the curve from the input bed level to the output bed level, and compares the output bed level to the corresponding Plymouth beach morphology survey. The trapezoid method is applied over a standardised area along the length of the profile, from easting reference 596505.3 to 596616.3 for all simulations on profile D. This method will infer changes in area under the curve to represent changes and movement in sediment on the beach. Results for profile B and G are provided in supplementary information 1, and reflect the results presented here.

The changes in area under the curve along the standardised section of profile D for the Plymouth beach morphology surveys are shown in Table 3. The Plymouth beach morphology survey records a loss of area [sediment] from 19 to 20 November 2016 (-3.41 %) in the lower energy conditions, and a gain in area [sediment] from 20 to 21 November 2016 (3.35%) on the higher energy conditions. There is an overall loss of area [sediment] over the 4 day survey period (-1.42 %).

Table 3: Sediment gains and losses (based on trapezoid method; area under curve) for a standardised length of profile D which includes the embedded Plymouth surveys from each date.

Scenario	Dates	Area	% change
	19	355.15	
	20	343.04	-3.41
	21	354.52	3.35
	22	350.11	-1.24
	Full week		-1.42

The change in area under the curve from the Plymouth beach morphology surveys are compared here to the changes seen during the four different calibration scenarios, detailed in Table 3. The area under the curve for scenarios where morphological evolution and sediment transport is turned OFF does not change and is the same at the start and at the end of the simulation, and so they are not included here.

Table 4 shows the area under the curve for scenarios with morphological evolution and sediment transport turned, where there is a movement of sediment onshore and offshore. The results are for the standardised section of profile D and show area under the curve at the start and end of the scenario, and then the % change over the duration of the scenario.

Scenario 1, during low energy conditions from 19 – 20 November, shows a loss of -2.24 % which reflects changes seen in the Plymouth beach morphology surveys from 19 to 20 November (-3.41 %). XBeach simulates a loss of -2.54 % area under the curve for scenario 2, during higher energy conditions from 20 – 21 November, which is not reflected by the Plymouth beach morphology surveys from 20 – 21 November where there is a gain in area (+3.35%). Over the duration of the survey period, XBeach simulates a greater loss of -3.92% than the Plymouth survey (-1.42%), as the model has not accounted for sediment gains during the higher energy storm conditions which were recorded in the surveys.

For the purpose of this section, scenario 1 was also run as with a fixed intertidal morphology. Table 4 shows that this approach substantially reduces sediment loss over the same period; low energy conditions cause a -0.42 % change in area when the offshore morphology is fixed compared to -2.24% change when it is not fixed. Similarly, higher energy conditions cause a -1.96 % change in area when the offshore morphology is fixed compared to -2.54% when it is not.

Overall the changes in the area under the curve reflect the lower energy conditions when sediment is lost from the beach, however XBeach is not able to accurately reflect sediment gains.

Table 4: Sediment gains and losses (based on trapezoid method; area under curve) for a standardised length of profile D from each XBeach scenario.

Scenario	Input area under curve	Output area under curve (morphology on)	% change from start to end
1	355.15	347.2	-2.24
2	343.04	334.34	-2.54
3	355.15	341.23	-3.92

4	343.04	336.33	-1.96
5	355.15	353.67	-0.42

2.2.5.3. Sediment size sensitivity testing

A sensitivity test was also completed on profile D to consider the influence of different sediment sizes on morphological evolution. Scenario 2 was re-run with a series of representative sediment size (see Table 5), and results are presented in Figure 8.

Table 5: Changes in sediment size in XBeach

	D50 (m)	D90 (m)
Default	0.0002	0.0003
Fine	0.0005	0.0007
Medium	0.0007	0.001
Coarse	0.001	0.002
Very Coarse	0.0025	0.00375
Mixed 1	0.0005	0.02
Mixed 2	0.0007	0.02

Figure 8 shows the input profile with the Plymouth beach morphology survey from the 20 November 2016 embedded into the CS_DEM as a black line, and the output bed level from 21 November 2016 for model outputs as coloured lines. The Plymouth beach morphology survey from the 21 November 2016 is shown as a purple line. Mixed sediment 1 and 2 show the greatest variation away from the input profile, with the morphology smoothed. Fine, medium, coarse, and very coarse show less infilling in the lows or smoothing of the highs. The coarse sediment size ("D50 = 0.001"; "D90 = 0.002") maintains the highs on the crests of the ridges, and does not infill the lows to the same extent as the mixed or finer sediments. For example, on the ridge located at easting reference 596576 the Plymouth 21 November survey is 1.27 m. The mixed sediment 1 size evolves the profile to 1.01 m, whereas the coarse sediment is at 1.22 m. At the low located at easting reference 596583 the Plymouth 21 November survey is at 0.99 m. The mixed sediment 1 infills so that the low is 1.3 m. The coarse sediment maintains the profile and the low is evolved to 1.02 m. The change in sediment size does not make a substantial difference to where erosion or deposition occurs, but does have an impact on the degree to which the profile is smoothed out.

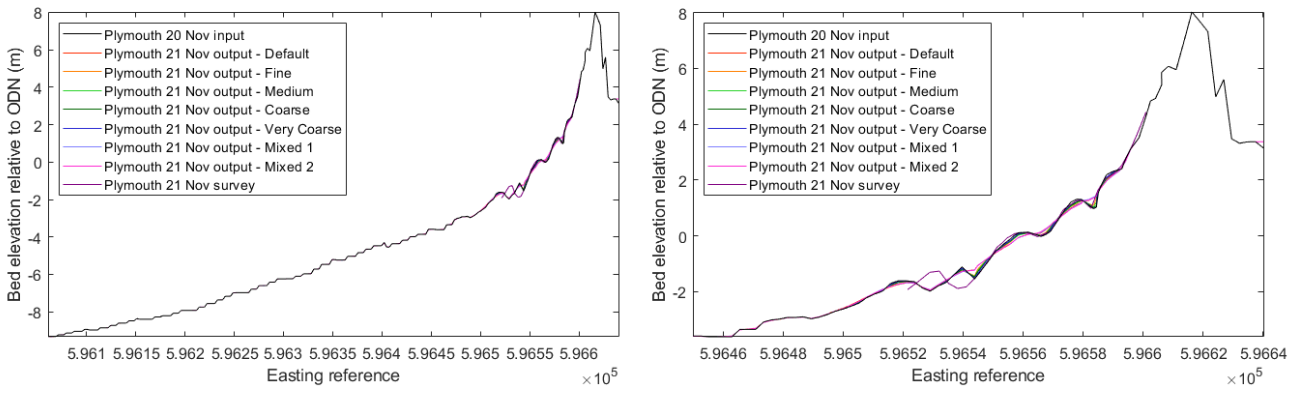

Figure 8: XBeach input and output profiles for 20-21 November 2016 scenarios under higher energy conditions with different sediment sizes including i) the CS_DEM with 20 November beach morphology survey embedded (black line); ii) 21 November beach morphology survey (purple line).

2.2.5.4. Wave runup time series:

A runup gauge was included with the "nrugauge = 1" keyword in the parameter file, to simulate and output wave runup on the profile every 60 seconds. A 15-minute running mean is applied to the model output data for baseline profiles, and profiles with the, with morphology on and off. The model outputs from profile B, D, and G are presented here against wave runup recorded by the pressure transducer deployed for the duration of Plymouth storm survey, which also has a 15-minute running means applied. The running mean makes the wave runup data more representative of the water level signal.

Figure 9 shows the wave runup time series for scenario 1 during low energy conditions. Wave runup on the baseline CS_DEM profile is shown with morphological development and sediment transport processes turned on (solid red line) and off (dashed red line). Wave runup on the profiles with the Plymouth beach morphology surveys embedded into the CS_DEM is shown with morphology on (solid blue line) and off (dashed blue line). Observation data from the pressure transducer is shown by the solid black line. There is little variability between the four model runs on profile D, which indicates less sensitivity to the input DEM and morphology switch here, however there is deviation from the observed wave runup at the time of high water. Wave runup shows greater sensitivity to input DEM and morphology switch on profile B and G. The profiles with Plymouth beach morphology survey embedded from 19 November and morphology turned off overestimate wave runup in profile B and G at the time of high water. The best agreement between model outputs and observation data at the time of high water is profile G, most notably when morphology switches are turned on. The error metrics in Table 6 also confirm good agreement between the model outputs and observation data. RMSE shows up to 1.38 m error, which is most notable on the ebb tide where there is greater variability as observed wave runup falls quicker than simulated wave runup. Overall there is good agreement between simulated and observed wave runup, which indicates that water level and wave outputs from the Met Office North West European Shelf seas model are accurate representations of local hydrodynamics and suitable boundary conditions for XBeach. For the purpose of this study, it is more important to accurately simulate wave runup at the time of high water when hazard may increase and when upper reaches of the beach and intertidal zone are covered and influenced by the tide. Data is not available from the pressure transducer at low tide as it was located above the level of low water.

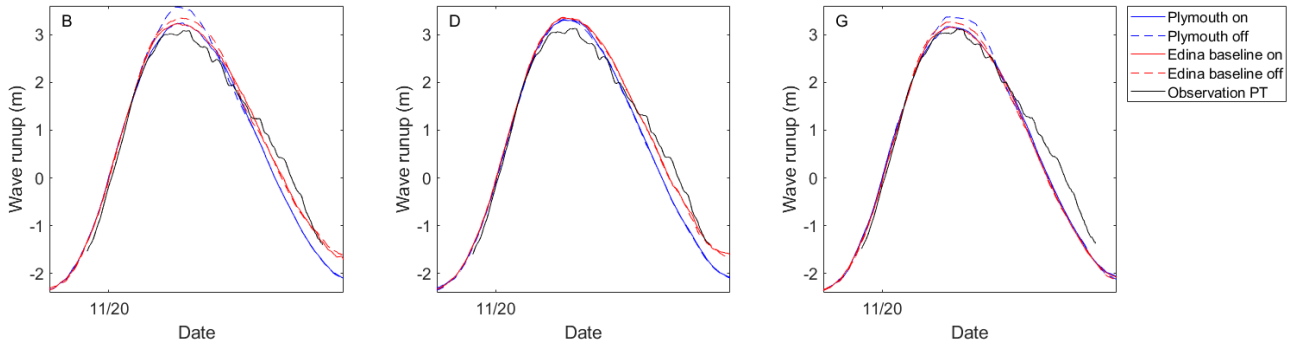

Figure 9: Scenario 1 simulated wave runup from 19 – 20 November 2016 showing Plymouth survey embedded in the Edina bathymetry with morphology and sediment transport i) on (blue solid line); ii) off (blue dashed line); and Edina LiDAR with morphology and sediment transport iii) on (red solid line); iv) off (red dashed line); and v) observation data for wave conditions from the closest pressure transducer (solid black line).

Table 6: Error metric coefficients (R^2, RMSE, Index of Agreement (Willmott, 1981; Willmott *et al.*, 2012) **values for low energy XBeach simulation from 19 – 20 November 2019 compared to Plymouth pressure transducer observation data.**

	Plymouth ON			Plymouth OFF			Baseline ON			Baseline OFF		
	R2	RMSE	IA	R2	RMSE	IA	R2	RMSE	IA	R2	RMSE	IA
B	0.97	1.38	0.99	0.97	1.38	0.98	0.99	1.38	0.99	0.98	1.38	0.99
D	0.97	1.39	0.99	0.97	1.39	0.99	0.99	1.39	0.99	0.99	1.39	0.99
G	0.97	1.38	0.99	0.97	1.38	0.98	0.97	1.38	0.99	0.97	1.38	0.99

Wave runup is presented in Figure 10 for the higher energy conditions, from 20 – 21 November 2016. Profile D shows least variability between the 6 XBeach simulations, and best agreement with the observation data from the pressure transducer. Profile B shows that the profiles with the Plymouth beach surveys embedded in the CS_DEM with morphology off and the fixed offshore morphology generate the most similar wave runup to the observation data. There is up to 0.22 m difference between the observed wave runup and the wave runup generated from the morphology on and baseline scenarios on profile B at the time of high water. XBeach exceeds observed wave runup up to 0.2 m on profile G when the morphology is turned off and when offshore morphology is fixed for the profile where 20 November 2016 Plymouth beach survey is embedded in the CS_DEM. Despite this, the R^2 and IA coefficients are close to 1 for all profiles and scenarios (Table 7), however RMSE exceeds 1.4 m due to the variability on the flood and ebb tide, and close to low water.

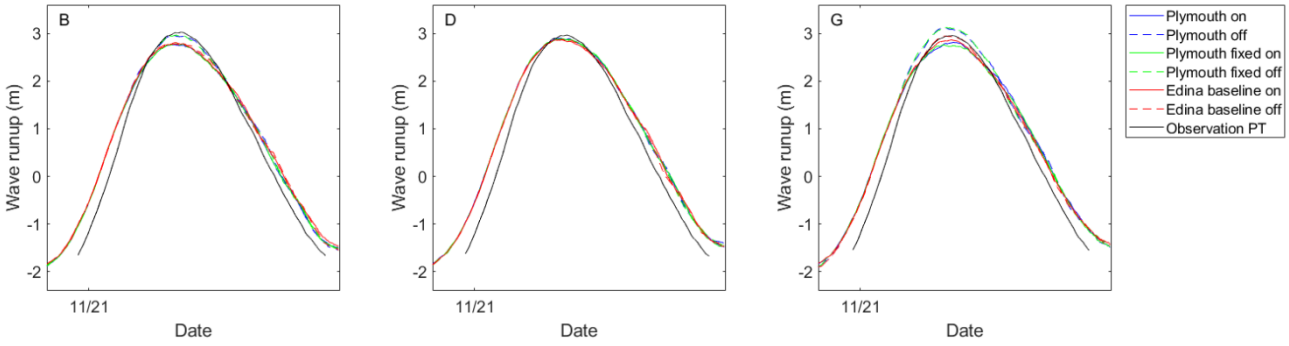

Figure 10: Scenario 2 and 4 simulated wave runup from 21 – 22 November 2016 showing Plymouth survey embedded in the Edina bathymetry with morphology and sediment transport i) on (blue solid line); ii) off (blue dashed line); iii) fixed intertidal zone with morphology and sediment transport iv) on (green solid line); v) off (green dashed line); Edina LiDAR with vi) morphology on (red solid line); vi) off; and vii) observation data for wave conditions from the closest pressure transducer (solid black line).

Table 7: Error metric coefficients (R^2, RMSE, Index of Agreement (Willmott, 1981; Willmott *et al.*, 2012) **values for low energy XBeach simulation from 20 – 21 November 2019 compared to Plymouth pressure transducer observation data.**

	Plymouth ON			Plymouth OFF			Baseline ON			Baseline OFF		
	R^2	RMSE	IA	R^2	RMSE	IA	R^2	RMSE	IA	R^2	RMSE	IA
B	0.99	1.46	0.99	0.99	1.46	0.99	0.99	1.46	0.98	0.99	1.46	0.98
D	0.99	1.45	0.98	0.99	1.45	0.98	0.99	1.45	0.98	0.99	1.45	0.98
G	0.99	1.45	0.98	0.99	1.45	0.98	0.99	1.45	0.98	0.99	1.45	0.98

	Plymouth Fixed ON			Plymouth Fixed OFF		
	R^2	RMSE	IA	R^2	RMSE	IA
B	0.99	1.46	0.99	0.99	1.46	0.99
D	0.99	1.45	0.98	0.99	1.45	0.98
G	0.99	1.45	0.98	0.99	1.45	0.98

There is variable agreement between the modelled and observed wave output during scenario 3; the 4 day scenario from 19 – 22 November 2016 (see Figure 11). Model outputs from four different setups consistently overestimate wave runup elevation on the second and third high water peak of the simulation. The Plymouth beach survey profile embedded in the CS_DEM with the morphology turned off consistently generates the largest overestimations of wave runup, up to 0.47 m higher than the observation recorded at the time of high water. The model outputs consistently underestimate wave runup at the peak of high water up to 0.3 m compared to the observation data on the first, fourth and fifth high water peak. There is no local influence in these scenarios, which could contribute to wave runup during higher energy conditions. The model outputs achieve good agreement on the sixth peak. The R^2 correlation coefficient is lower for scenario 4 across all profiles, as the record is longer and more opportunity for inconsistencies (Table 8). Further to this, the pressure transducers do not record the low tides, so there is no data to compare the model simulations to at these points. The RMSE and IA are in a similar range to the error metrics seen for scenario 1,2 and 4. Over several tides it is evident that outputs from the Met Office North West European Shelf seas model are suitable to use as water level and wave boundary conditions for XBeach.

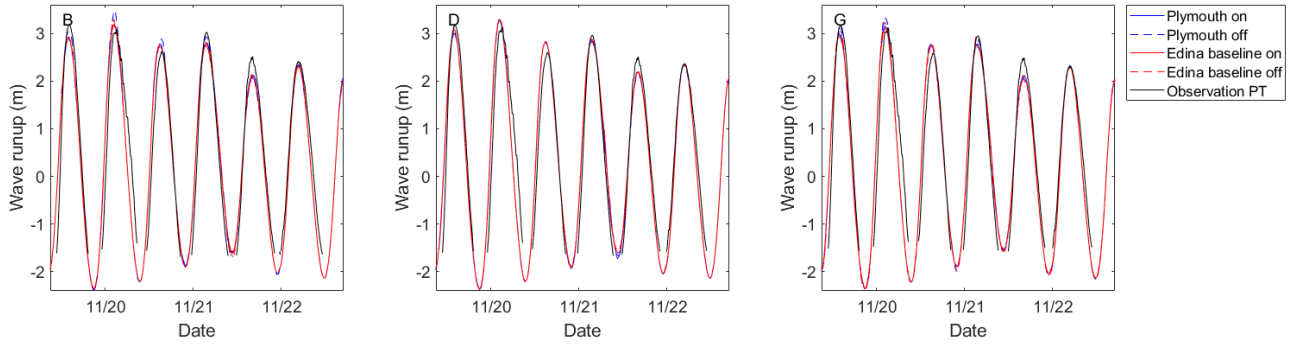

Figure 11: Scenario 4 simulated wave runup from 21 – 22 November 2016 showing Plymouth survey embedded in the Edina bathymetry with morphology and sediment transport i) on (blue solid line); ii) off (blue dashed line); Edina LiDAR with morphology and sediment transport iii) on (red solid line); vi) off; and v) observation data for wave conditions from the closest pressure transducer (solid black line).

Table 8: Error metric coefficients (R^2, RMSE, Index of Agreement (Willmott, 1981; Willmott *et al.*, 2012) **values for low energy XBeach simulation from 19 – 22 November 2019 compared to Plymouth pressure transducer observation data.**

	Plymouth ON			Plymouth OFF			Baseline ON			Baseline OFF		
	R^2	RMSE	IA	R^2	RMSE	IA	R^2	RMSE	IA	R^2	RMSE	IA
B	0.89	1.33	0.97	0.89	1.33	0.97	0.88	1.33	0.97	0.88	1.33	0.97
D	0.89	1.32	0.97	0.89	1.32	0.97	0.88	1.32	0.97	0.88	1.32	0.97
G	0.88	1.28	0.97	0.88	1.28	0.97	0.88	1.28	0.97	0.88	1.28	0.97

The model calibration and validation has focused on the model's ability to simulate morphological evolution and wave runup over time, and how the model is sensitive to different bathymetry. The level of confidence on the morphological modelling, as a time series or a before and after, is quite low. The model smooths the morphology during the simulations, but still captures the general slope of the beach. Although that confidence is low, there is a good level of confidence in the wave runup modelling which shows that the model can represent observed wave runup values compared to values recorded using a pressure transducer. This gives confidence in model capabilities for the purpose of the next section of this study. The model has also been calibrated in respect to sediment size for future scenarios.

3. Assessment of wave runup hazard

Wave runup has been successfully against storm surveys from Plymouth which gives confidence in relation to its application for the next section of the study, where the sensitivity of wave runup to X-band radar-derived intertidal morphology is explored. The following section describes how the X-band radar-derived intertidal morphology and boundary conditions were processed for the period when the radar tower was operating at Camber Sands from 16 November 2018 – 30 June 2019. The quality of images from the radar are only continuous to produce reliable intertidal morphologies from the 19 March 2019 to 30 June 2019.

The sensitivity of wave runup simulated by XBeach to different DEMs is explored over the course of a historic storm event that represents a period of high energy, wave conditions. This is so that the radar can identify the sea surface more clearly, and subsequently generate a more accurate DEM in post-processing, and also so that an event is simulated which represents a potential hazard at the coast and produces substantial waves at the coast. Total water level and significant wave height were downloaded from the Met Office North West European Shelf seas model, from the E.U. Copernicus Marine Service (Clementi et al., 2019) for the period the radar was operating from 19 March 2019 to 30 June 2019 (see Figure 12). The largest significant wave height during this record is identified as 2.4 m on 8 June 2019 13:00. This significant wave height is combined with WL, 3.14 m, to generate a high water hazard proxy (HWHP) calculated as WL + ½ Hs, often used by coastal managers as a representation as a coastal condition of 4.34 m. The HWHP is shown as black dots in Figure 12, and the event selected represents one of the highest HWHP in this record.

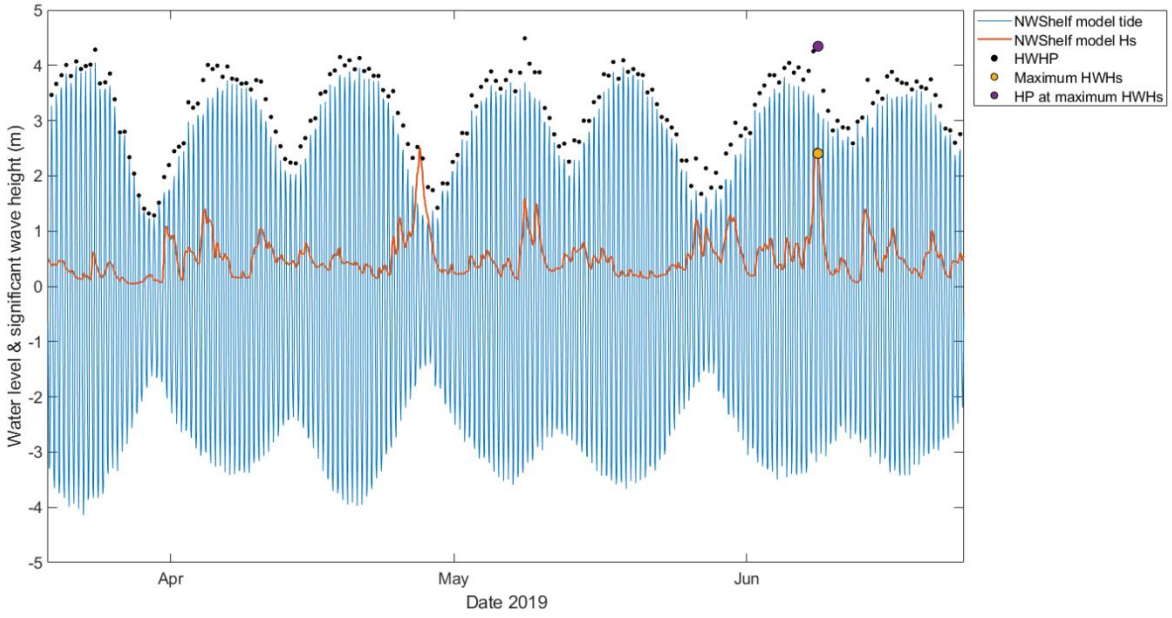

Figure 12: Water level (blue line) and significant wave height (red line) record from the UK Met Office North West European Shelf seas model from 19 March 2019 to 30 June 2019 when the radar tower was operating. HWHP (black dots) is calculated for the record. Maximum HWH_s (yellow dot), and maximum HWHP (purple dot) is shown for the 8 June 2019 13:00 storm event.

3.1. Digital Elevation Model from X-band radar

Data used in this study were gathered using a standard X-band marine radar operating from 16 November 2018 – 30 June 2019. The accuracy and coverage of the X-band radar-derived intertidal morphologies is dependent on obtaining a complete water level signal. The temporal waterline algorithm (Bell *et al.*, 2016) was applied using local Met Office North West European Shelf seas model outputs at an hourly temporal resolution. The X-band radar intertidal morphologies processed from local Met Office North West European Shelf seas modelled water level outputs (XBR_DEM_NWS) was further processed using 1, 5 or 10 day averaging period.

3.1.1. X-Band radar-derived intertidal morphologies

Marine radar images were temporally averaged over a set period to show the mean elevation of the radar-observed waterline over that period, and an approximation of the mean elevation of the intertidal morphology (see Bird *et al.*, 2017). Marine radar images were processed over a 1, 5, and 10 day averaging windows in the run up to the 8 June 2019 storm event (see Table 9). The three different averaging windows will show how the coverage and resolution of X-band radar-derived intertidal morphology varies when generated from observations over different set periods. A longer period was expected to improve the resolution and coverage of the X-band radar-derived intertidal morphology as there is improved chance of waves on the sea surface to improve accuracy of the waterline mapping technique. However, larger changes in the intertidal zone may take place during this period which may lead to a summation of variable morphology for the longer periods of observation.

Table 9: X-band radar-derived intertidal morphology averaging windows

Averaging window (days)	Start	End

1	07.06.2019 00:00	07.06.2019 23:50
5	03.06.2019 00:00	07.06.2019 23:50
10	29.05.2019 00:00	07.06.2019 23:50

The radar-derived intertidal morphologies are provided as an ASCII file, and are converted to raster format in ArcMap. The different averaging windows, which represent averaged changes in the intertidal zone, are shown in 3 DEMs: 1, 5, and 10 days. Figure 13 shows the 10-day averaged XBR_DEM_NWS, and Appendix 1 and 2 show the 1- and 5-day XBR_DEM_NWS for comparison. These three DEMs are used to assess the application of X-band radar-derived nearshore topographic-bathymetric data as input for process-based models, to characterise coastal system behaviours, as well as exploring the optimal duration of radar data required to detect changes in intertidal bathymetry due to the prevailing hydrodynamic forcing.

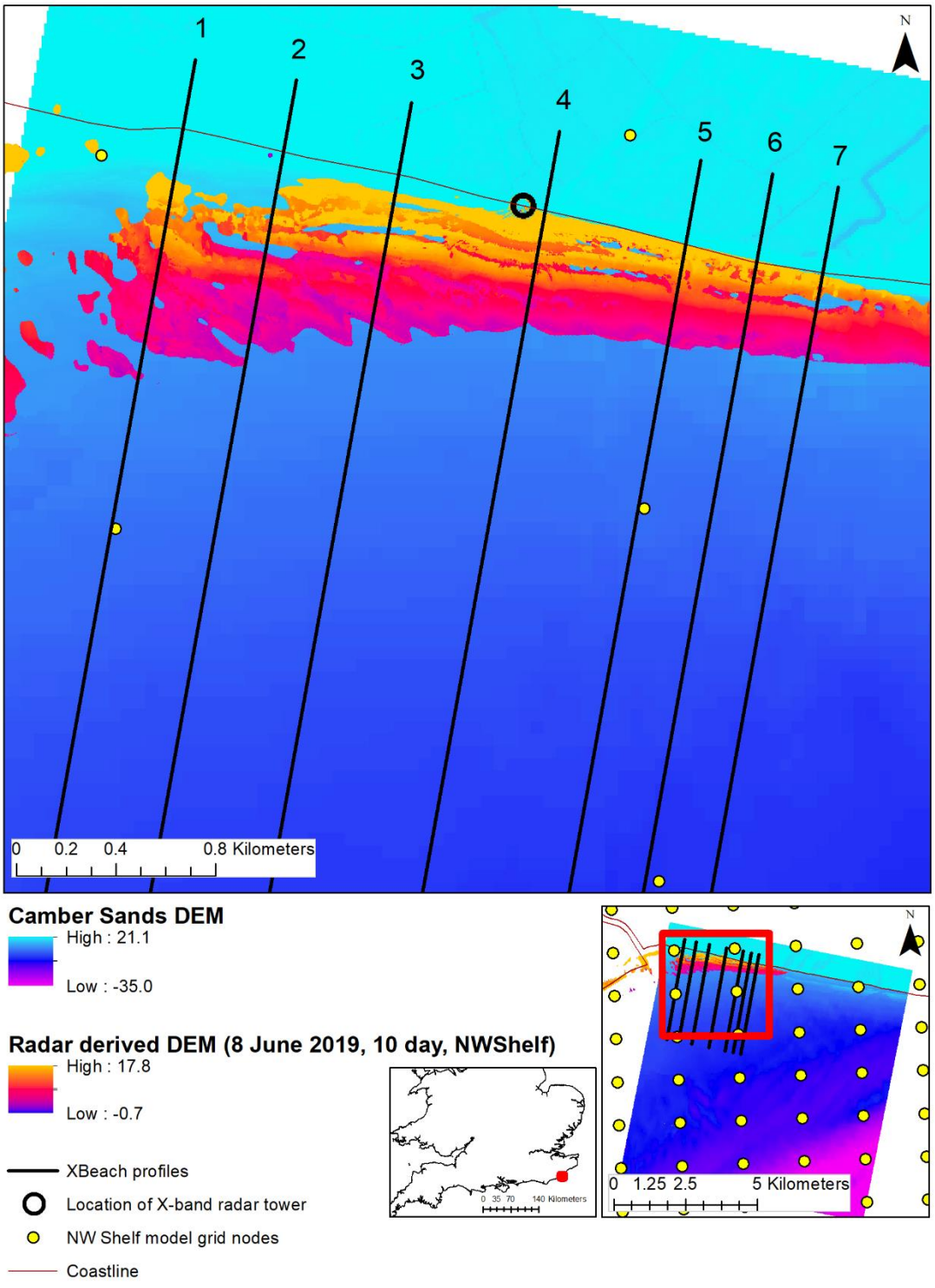

Figure 13: CS_DEM, generated from LiDAR data, in addition to 10-day XBR_DEM_NWS.

Appendix 3 shows the 10-day XBR_DEM_NWS on Profile 4 and a series of cross-shore beach profiles at Camber Sands taken from LiDAR surveys conducted between 2000 – 2020 and beach profile surveys from the Channel Coastal Observatory (CCO, 2020). This demonstrates the variability in the profile from different data sources, and that the X-band radar-derived intertidal morphologies may be variable but still represent average beach slope.

3.2. Radar-derived cross-shore beach profiles

Seven parallel, cross-shore beach profiles were investigated in the wave runup assessment, numbered 1-7, which were located dependent on where there is high coverage from the XBR_DEM_NWS (Figure 13). These profiles were different to the profiles used in the calibration and validation study. Each profile is 3.5 km, and the offshore limit represents the location at which the offshore boundary conditions are applied from the Met Office North West European Shelf seas model grid node *50.9054, 0.7878* and *50.9054, 0.8181*. This is the same as used in the calibration and validation study. Elevation data is extracted from the CS_DEM at a resolution of 5 m and used as a baseline. The three XBR_DEM_NWS only cover a section of the intertidal zone, so were extended offshore with the CS_DEM to determine the sub-tidal gradient, and elevation data was also extracted at a 5 m resolution.

3.2.1. Idealised slope of profile

Elevation data along cross-shore beach profile 4 from the CS_DEM is shown as a solid black line in Figure 14i. Coloured lines in Figure 14ii, iii, and iv show elevation data along the cross-shore beach profile extracted from each of the 1-, 5-, and 10-day XBR_DEM_NWS. The XBR_DEM_NWS show considerable variability and are raised above the level of the CS_DEM despite their lower limit aligning with the baseline topography. The sharp changes in bed level (up to 3 m in places) were not representative of the beach morphology and caused errors when simulating wave runup in XBeach and model runs did not finish. A straight line is drawn through the profiles to represent the average beach slope. An idealised beach slope was first generated from the CS_DEM, termed Camber Sands idealised slope (CS_IS) and used as a baseline. The radar-derivedidealised beach slopes processed from Met Office North West European Shelf seas modelled water level outputs (XBR_IS_NWS) were positioned radar-derivedso that the straight line is representative of the beach slope by crossing peaks in the profile. Topographic highs are likely to be better resolved by the radar as opposed to lows where line-of-sight shadowing can occur. The three XBR_IS_NWS are at similar angles to each other but are steeper than the CS_IS. The representative average beach slope for each X-band radar-derived profile is embedded in the CS_DEM to extend it offshore and processed in Matlab to generate .dep files to input into XBeach. Wave runup simulations have been validated in XBeach, so there is high confidence in using idealised beach slopes to determine runup hazards.

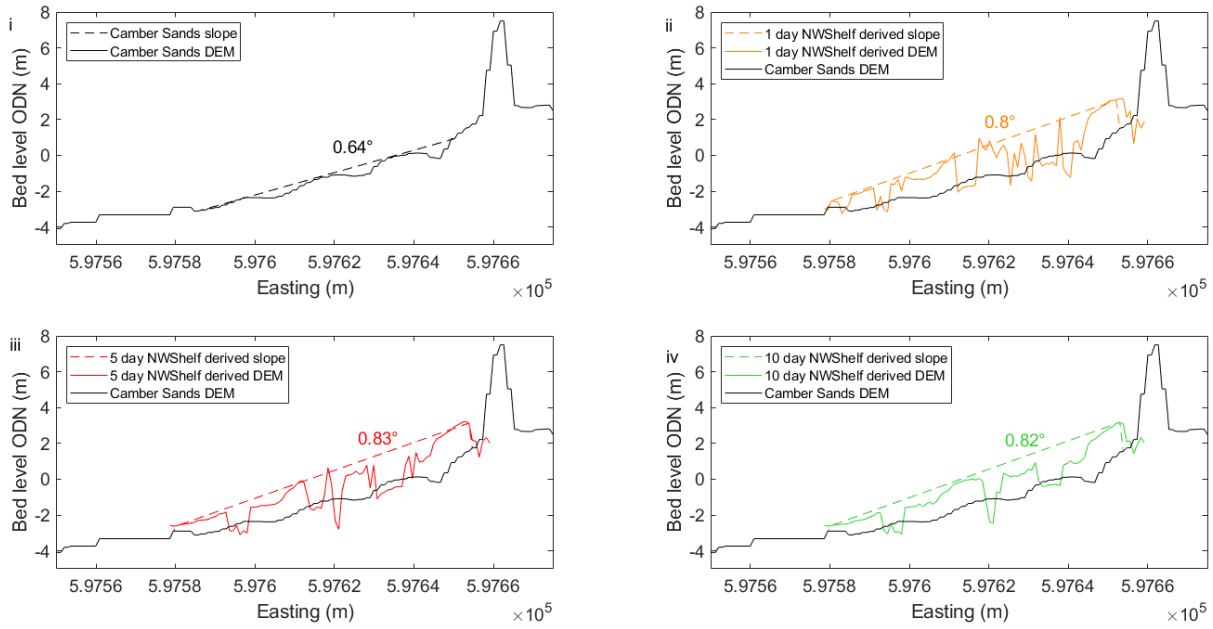

Figure 14: 2DH cross-shore beach profiles (solid line) and idealised beach slope (dashed line) along cross-shore profile 4 for i) CS_DEM and CS_IS; ii) 1; iii) 5; iv) 10 day averaged XBR_DEM_NWS and XBR_IS_NWS.

3.2.2. Boundary conditions

As with the calibration and validation study, outputs from the Met Office European North West Shelf Model, using the E.U. Copernicus Marine Service (Clementi et al., 2019), were used as boundary conditions. Model outputs from January 2017 onwards are available for direct download in netCDF format from the E.U. Copernicus Marine Service. Hourly water level (relative to the geoid) and wave parameters (Hs, Tp, Dir) were downloaded and processed in Matlab to generate input files for XBeach. The Met Office North West European Shelf seas model outputs are used here to represent the local water level, from grid nodes at *50.9054, 0.7878* and *50.9054, 0.8181*. An hourly water level time series (tide + surge) is used to force the offshore boundary of each profile (*zs0file = tide.txt; tideloc = 1*). The wave characteristic time series from WAVEWATCH III are used to create a JONSWAP spectra, with the jonstable switch (*instat = 4; bcfile = bcfile.txt*), providing wave height, peak period, direction, spreading every hour at the offshore boundary.

3.3. Model scenarios

XBeach simulations were run for storm event from 07/06/2019 13:00 to 08/06/2019 21:00 across each of the seven profiles (numbered 1 – 7) from CS_DEM, CS_AS, and each of the averaged XBR_IS_NWS. The model scenarios are shown in Table 10; 10 scenarios are run for each profile, and 70 simulations completed in total. The model is run with morphological evolution and sediment transport turned on and off, to test the sensitivity of wave runup hazard to this parameter.

Table 10: Model scenarios

DEM	Morphological evolution and sediment transport
Camber Sands DEM (CS_DEM)	0 / 1
Camber Sands idealised slope (CS_IS)	0 / 1

1-day XBR_IS_NWS	0 / 1
5-day XBR_IS_NWS	0 / 1
10-day XBR_IS_NWS	0 / 1

Water level (zs), water depth (hh), Hrms wave height based on instantaneous wave energy (H), and bed level (zb) were saved every minute. A runup gauge was used (nrugauge = 1) to output wave runup at 60 s intervals. The sensitivity of high water wave runup to input conditions for each simulation is presented in a series of figures including i) time series over the peak of high water; ii) maximum wave runup at the time of high water; and iii) area under the curve.

4. Results

4.1. Wave runup time series (7 plots with 15 minute running mean applied)

XBeach was run on seven cross-shore profiles, from high tide before the storm event to low tide after the storm event (07/06/2019 13:00 to 08/06/2019 21:00), on 5 different DEMs to test the sensitivity of wave runup to changes in DEM and morphological switches. A runup gauge was used to record the elevation of wave runup in the intertidal zone, and model outputs were saved at 60 s intervals. A 15 minute running mean was applied to the wave runup model outputs to clear the tidal influence, and more clearly present wave runup sensitivity over the peak of HW.

Figure 15 shows the sensitivity of wave runup for each of the seven cross-shore profiles to changes in DEM and morphological switches. Wave runup over the peak of HW at each cross-shore profile shows a different degree of sensitivity to changes in the DEM and morphological switch, which may reflect changes in elevation along each profile. Wave runup on profile 1 and 2, located furthest west on Camber Sands, show least sensitivity to changes in DEM and morphological switch on the flood and ebb tide, and at the time of HW. Wave runup sensitivity increases on the profiles to the east, towards Broomhill Sands. The model simulates variability in wave runup at profile 3 at the time of HW, as CS_DEM, CS_IS, 1-day XBR_IS_NWS with morphological evolution and sediment transport processes are turned on generate smaller wave runup at HW. The model generates greatest sensitivity of wave runup at HW to different DEMs on profile 4; CS_DEM and CS_IS generates smaller wave runup at HW with the morphological evolution and sediment transport processes turned on and off compared to all XBR_IS_NWS. XBeach generates variability in wave runup at HW on profile 5, 6, and 7, but there is no consistency as to which DEM generates the largest runup.

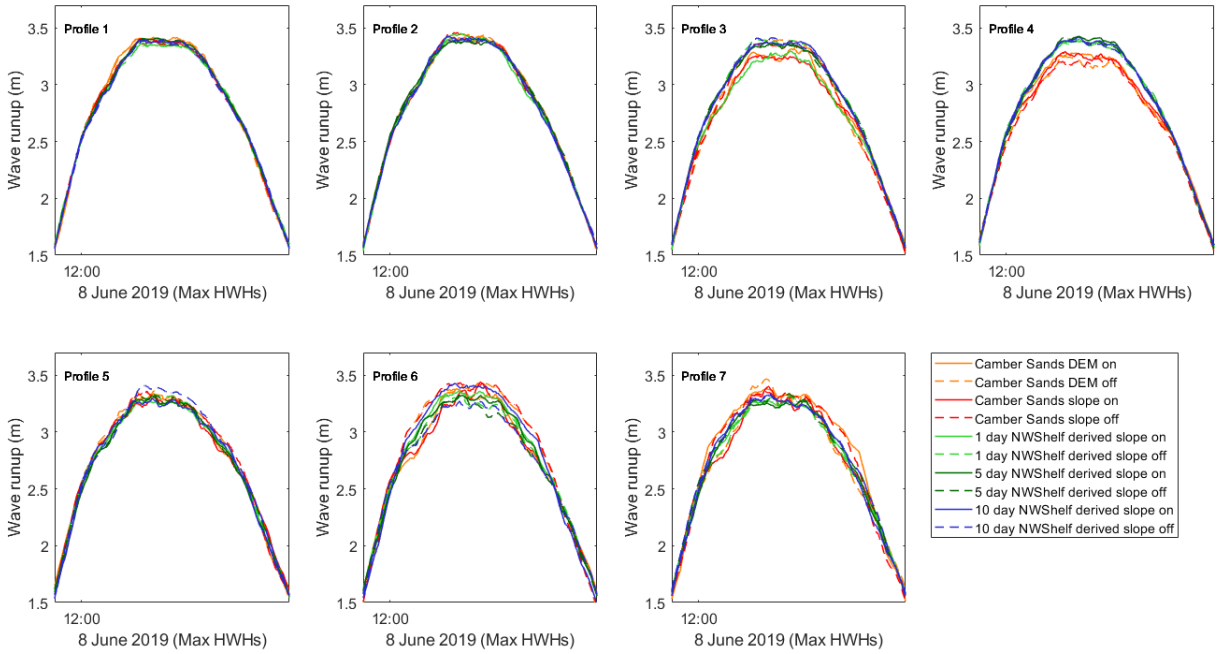

Figure 15: Simulated wave runup outputs from XBeach for each DEM or input idealised slope with morphological evolution and sediment transport on or off during high water conditions, with a 15 minute running mean applied for each cross-shore beach profile from CS_DEM, CS_IS, and XBR_IS_NWS.

4.2. Max WR and at time of HW

Figure 16 shows the maximum wave runup at the time of HW (8 June 2019 13:30) for each of the seven cross-shore profiles (along the x-axis). The model simulates largest wave runup at the time of HW on profile 1 (3.4 m) and profile 2 (3.42 m), but the model also generates just 0.06 m range of wave runup values at the time of high water on these profiles. The model generates much larger range of wave runup at the time of high water for the remaining profiles to the east; up to 0.25 m on profile 4. Figure 16 also shows that the model generates a 0.07 m difference in wave runup at the time of HW on profile 4 between simulations from the CS_DEM, CS_IS, and XBR_IS_NWS.

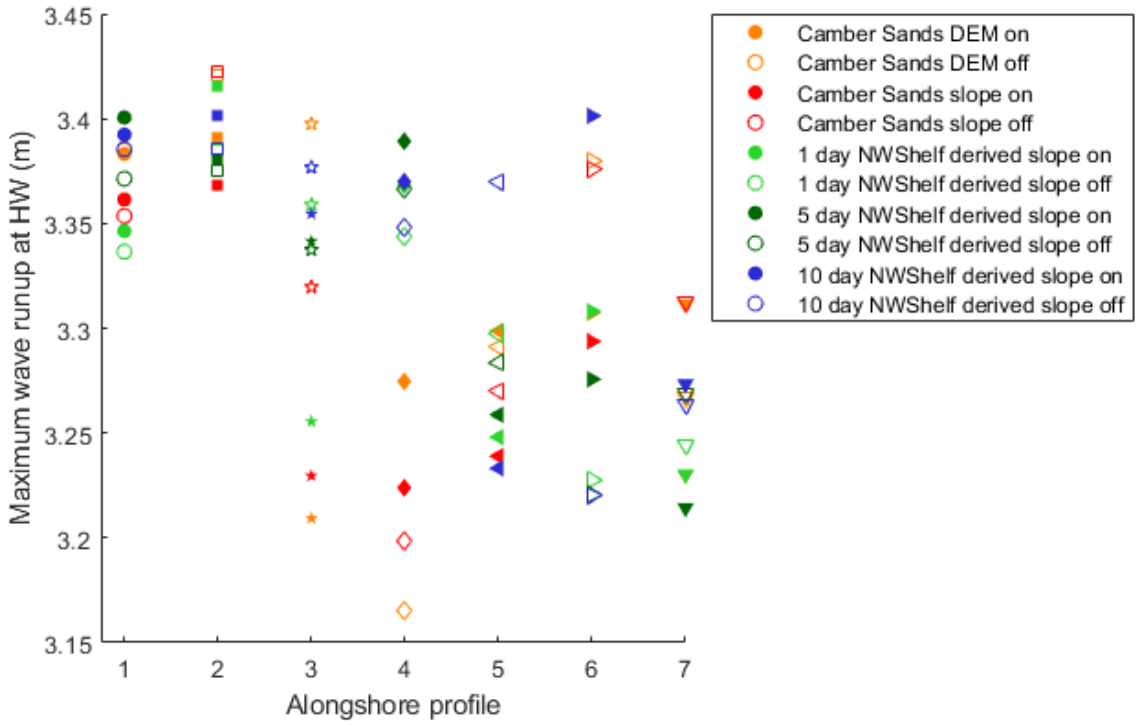

Figure 16: Maximum simulated wave runup at the time of high water (8 June 2013 13:00) for each input DEM with morphological evolution and sediment transport on or off.

4.3. Area under curve

Figure 17 shows the area under the curve (metres *x* seconds) of the HW peaks (shown in Figure 17), calculated using the trapezoid method, for each model simulation completed on the seven cross-shore profiles. This analysis captures how the different DEMs may alter wave runup on the flood and ebb tide, to influence the steepness on the rising and falling limb of the tide and subsequent peakedness of the time-series curve. Profile 1, 2, 3, and 6 show smallest area under the curve, as the model generates smaller maximum wave runup elevations and the peak of the time-series is narrower. Profile 4, 5 and 7 show greater variability in area under the curve, but little consistency as to which model simulation generates the greatest area.

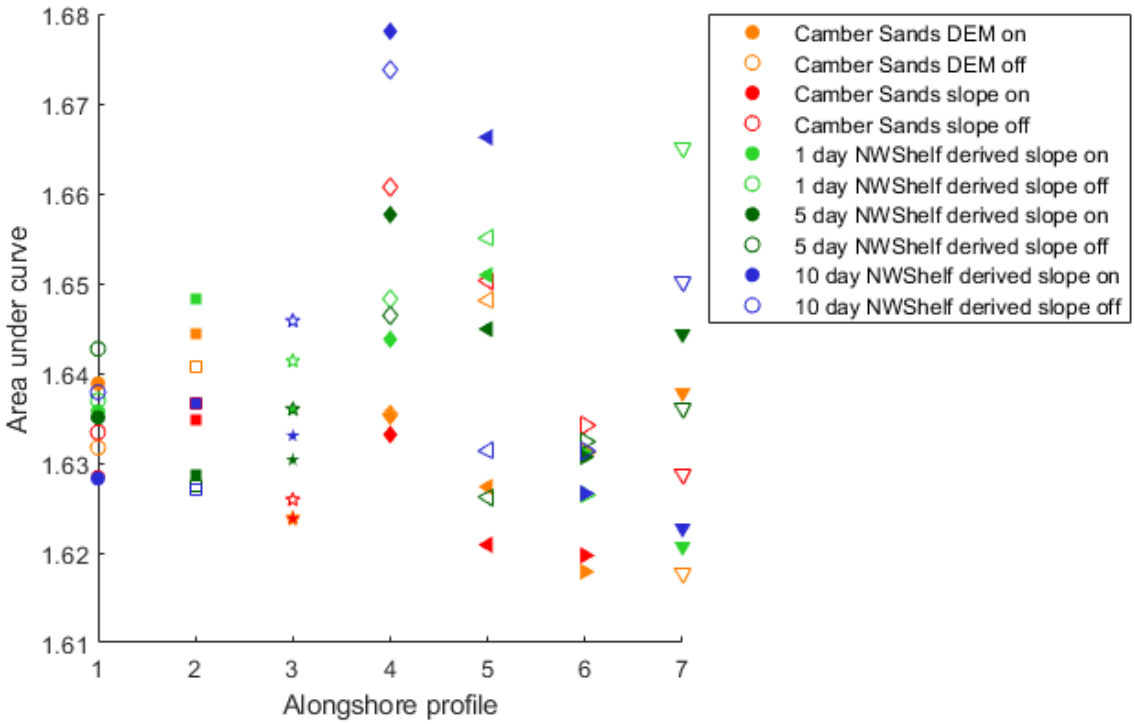

Figure 17: Area under the curve during high water conditions for CS_DEM, CS_IS, and XBR_IS_NWS with morphological evolution and sediment transport on or off.

4.4. Tide gauge versus local model data

Figure 15 confirms that the model shows greatest sensitivity to variability in intertidal morphologies on profile 4. The model generates smaller maximum wave runup at the time of high water on the CS_DEM and the CS_IS, compared to XBR_IS_NWS. The results presented so far use water level data taken from the Met Office North West European Shelf seas model in the temporal waterline algorithm, to generate a DEM and idealised slope. The water level time series used in the waterline algorithm to generate the X-band radar-derived DEMs is a local record of water level, taken from a model a grid node local this case study. In this instance, the water level record generated a more variable DEM.

The waterline algorithm was re-run using a regional record of water level, from the Dover tide gauge located at the Prince of Wales Pier, Western Dock (*51.1151, 1.3224)*, to consider the influence of water level record on the waterline algorithm, and the subsequent DEM. Figure 18 shows the regional total water level (tide + surge) record from Dover tide gauge and the local total water level from the Met Office North West European Shelf seas model between 1 May 2019 and 1 July 2019, the period when the storm event simulated here is included in. The regional water level record from Dover tide gauge has a similar phase to the Met Office North West European Shelf seas model outputs, but smaller tidal range. The Dover tide gauge records a lower high water level and a higher low water level. The difference in high and low water elevation in the record will have an influence on the waterline method used to generate the X-band radar-derived DEMs. The difference in tidal range will influence where the shoreline is placed, and subsequently the overall position, slope, and detail of the DEM.

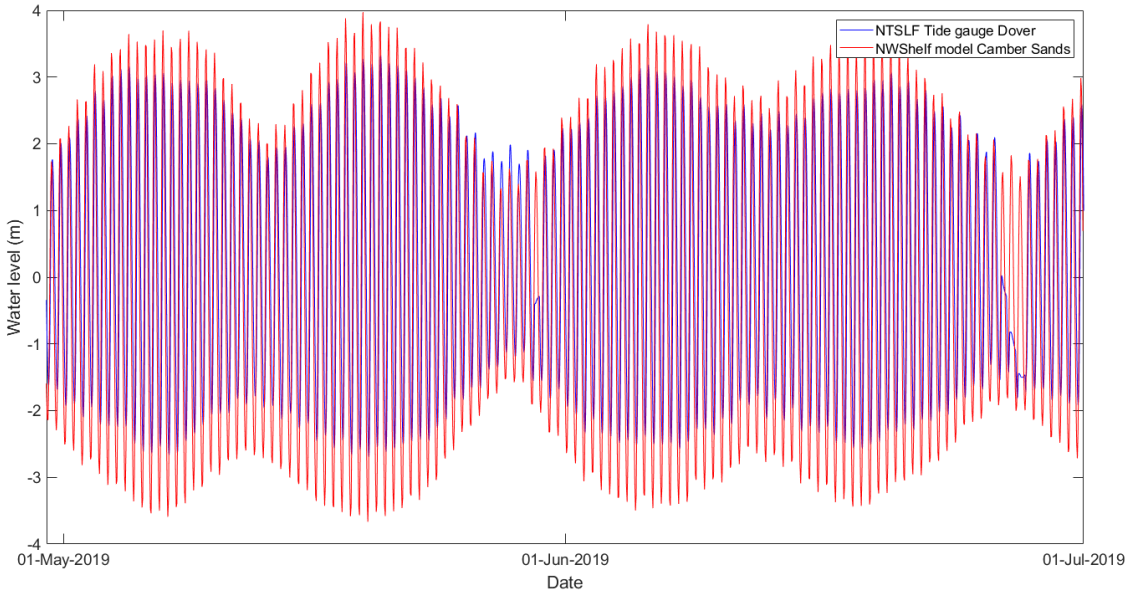

Figure 18: May – June 2019 water level record from the NTSLF tide gauge located at Dover, and the Met Office North West European Shelf seas model grid node at Camber Sands.

4.4.1. Influence of waterline method on DEM

The 10-day averaged X-band radar-derived DEM processed from regional Dover tide gauge observation water level (XBR_DEM_DOV) is shown in Figure 19. The extent of the DEM is like that seen in Figure 13, however there is a greater coverage of data to the west at the Camber Sands sand dune system.

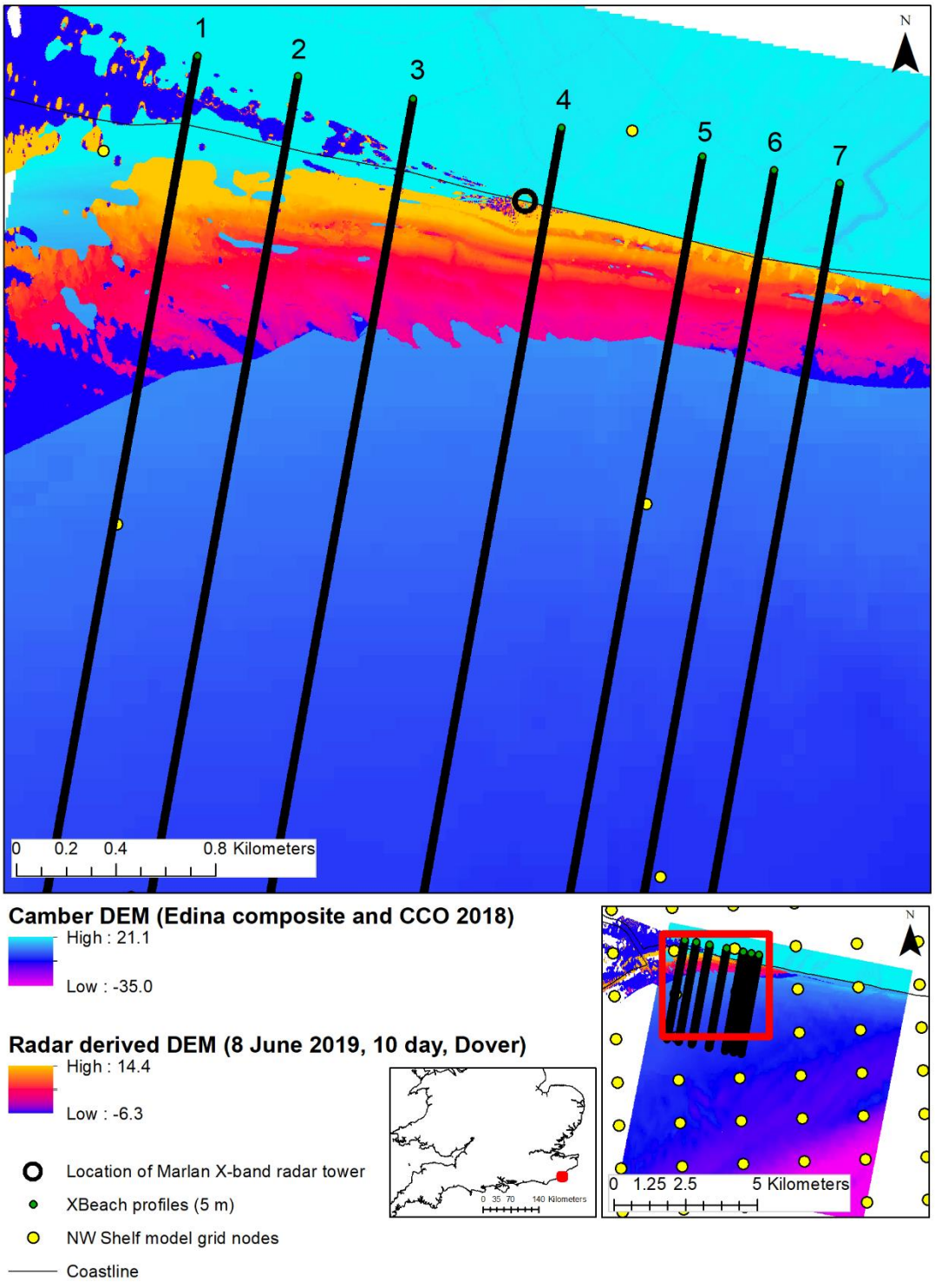

Figure 19: CS_DEM, generated from LiDAR data, in addition to 10 day averaged X-band radar-derived DEM processed from regional Dover tide gauge observation water level (XBR_DEM_DOV).

An idealised slope is also applied to the XBR_DEM_DOV, so that modelled wave runup can be simulated and compared on the X-band radar-derived idealised slope processed from regional Dover tide gauge observation water level (XBR_IS_DOV) and compared to XBR_IS_DEM.

Figure 20 shows the cross-shore elevation change at profile 4 from all DEMs; CS_DEM, CS_IS; XBR_DEM_NWS; XBR_IS_NWS; XBR_DEM_DOV; XBR_IS_DOV. There is a greater level of resolution and less variability within XBR_DEM_DOV. The morphology of the profile appears smoother and there is a more clearly defined ridge runnel system. The XBR_DEM_DOV are elevated above the level of the CS_DEM which could be due to accumulation on the beach since the LiDAR surveys, or the Dover tide gauge under-recording how low the low water gets. There is some distortion on the XBR_DEM_DOV towards the upper beach, notably on the 10 day averaged DEM, which could be due to shadowing, but will be cropped from the XBeach input profile. Further to this, the XBR_DEM_DOV record more clearly shows how a longer averaging window can improve the resolution of the DEM, but also how it marginally increases the slope angle.

The idealised beach slope is lowered in all XBR_IS_DOV (blue dashed line in Figure 20), derived from the XBR_DEM_DOV. As seen in Figure 20, the Dover tide gauge is not as high at high water and not as low at low water as the UK Met Office North West European Shelf seas model outputs, therefore the waterline algorithm places the high tide shoreline at a lower elevation, and the low tide shoreline at a higher elevation. This generates a shallower profile. The Dover outputs are higher resolution and show better coverage, so it could be assumed the XBR_DEM_DOV are more accurate. However, the regional water level record from the Dover tide gauge shows up to a 2.5 m smaller tidal range which is not representative of local conditions at Camber Sands. Therefore the next section of will consider which water level record is best to use in the waterline algorithm to use in XBeach for accurate wave runup assessment.

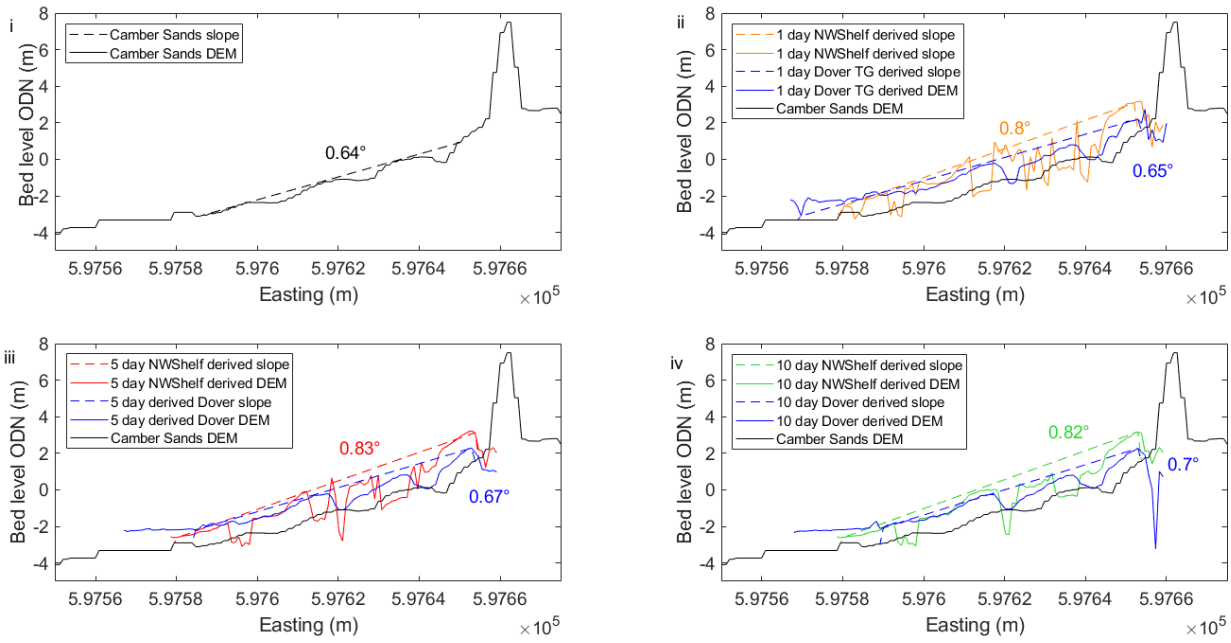

Figure 20: 2DH cross-shore beach profiles (solid line) and idealised beach slope (dashed line) along cross-shore profile 4 for i) CS_DEM and CS_IS; ii) 1 ; iii) 5; iv) 10 day averaged XBR_DEM_NWS / XBR_IS_NW (orange; red; blue) and XBR_DEM_DOV / XBR_IS_DOV (blue).

4.4.2. Influence on Wave Runup

XBR_IS_DOV is used as input to XBeach on profile 4 on the 8 June 2019 storm event, to explore the influence of lower slope level, due to different water level records used in the temporal waterline

algorithm, on simulated wave runup. Simulated wave runup is shown over the peak of high water in Figure 21a-c. A 15 minute running mean is applied to each wave runup record.

Smaller wave runup is consistently generated by 1-, 5-, and 10-day XBR_IS_DOV on the shallower average beach slopes over the peak of high water, compared to XBR_IS_NWS. Wave runup shows little sensitivity to the morphological evolution and sediment transport switch.

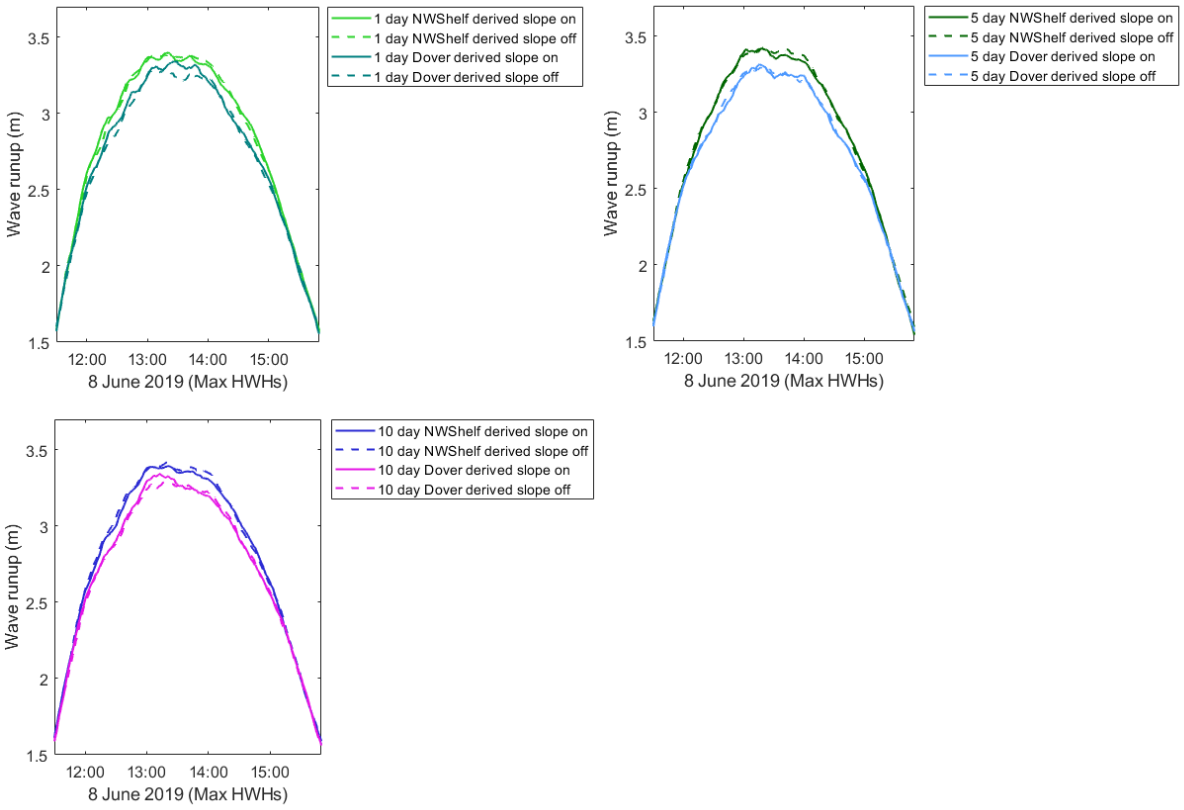

Figure 21: Simulated wave runup outputs from XBeach along cross-shore profile 4 from XBR_IS_DOV and XBR_IS_NWS, with morphological evolution and sediment transport on or off during high water conditions.

The simulated wave runup outputs 1-, 5-, and 10-day XBR_IS_DOV are shown alongside outputs from CS_DEM, CS_IS, and XBR_IS_NWS in Figure 22. XBR_IS_DOV simulations bring the modelled wave runup in line with the results from the CS_DEM and CS_IS, indicating it may be more reliable to use the instrumented and recorded tide gauge water level to process the X-band radar outputs, compared to water level outputs from the Met Office North West European Shelf seas model. As seen in Figure 22, the UK Met Office North West European Shelf seas model outputs are not substantially over-predicting high water level at Dover when compared to the instrumented tide gauge record from Dover. There is discrepancy in the UK Met Office North West European Shelf seas model outputs and Dover tide gauge at low water, however this could be because the tide gauge is raised above the seabed and not fully capturing low water.

This indicates that there is no error in the UK Met Office North West European Shelf seas model outputs, but the instrumented tide gauge produces a shallower sloped DEM with greater resolution and coverage, which, when used as an input in XBeach, generates a wave runup that is more in line with the outputs from the CS_DEM, used here as a baseline.

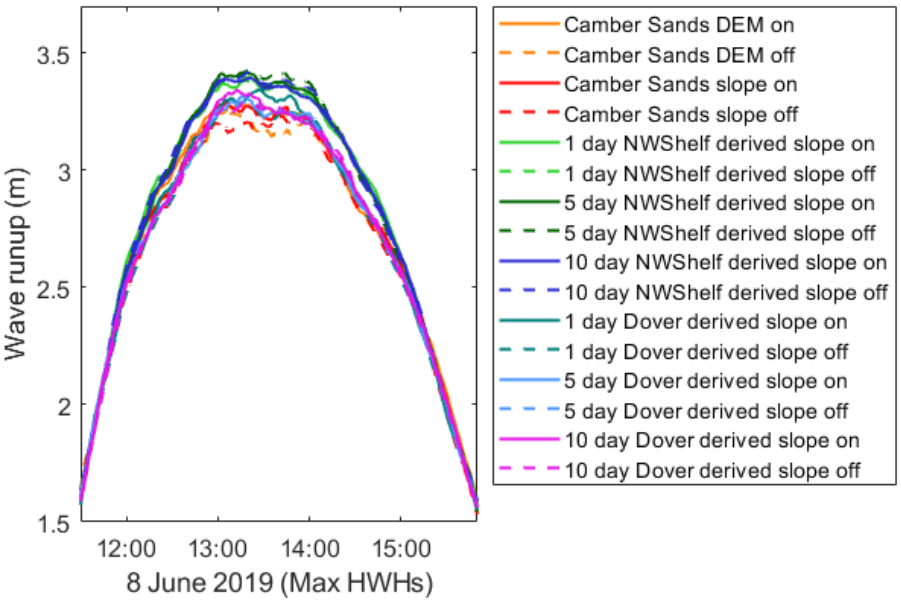

Figure 22: Simulated wave runup outputs from XBeach along cross-shore profile 4 from the CS_DEM, CS_IS, XBR_DIS_NWS, and XBR_IS_DOV, with morphological evolution and sediment transport on or off during high water conditions.

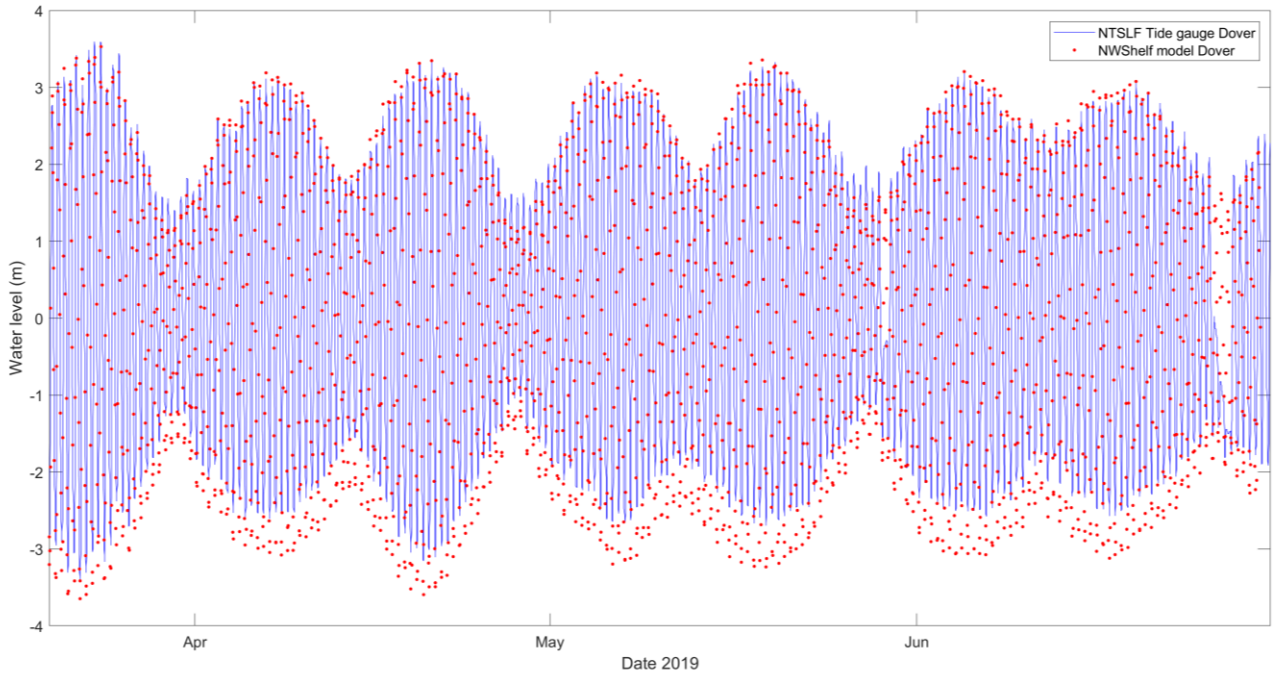

Figure 23: Comparison of the Met Office North West European Shelf seas model outputs from the same location as the Dover tide gauge from 19 March 2019 to 30 June 2019.

5. Discussion

The strategic management of flood and erosion hazards at the coast rely on a thorough and accurate understanding of ongoing coastal processes at a range of temporal and spatial scales. Robust tools are needed to record shoreline changes in response to high-energy, storm conditions to inform current and future predictions of coastal risks. Shore-based, marine navigational radar operating at X-band frequency has previously been used to characterise coastal behaviours over a range of timescales (Bird et al., 2017; Atkinson et al., 2018). This research assesses the application of X-band radars for deriving nearshore topographic-bathymetric surveys and wave runups in process-based model XBeach. XBeach has been widely used as a tool for storm hazard prediction and morphological change (Bird *et al.*, 2017) and is used here to simulate wave runup at Camber Sands, southeast England, which is a shallow sloping sandy beach.

Sensitivity of modelled wave runup

XBeach was forced with outputs from the Met Office North West European Shelf seas model and calibrated to beach morphology surveys completed at Camber Sands in November 2016. The model gives low confidence in morphological development along two-dimensional, horizontal profiles as no account is made for alongshore sediment transport and wind. Low confidence in morphological development of each 2DH cross-shore beach profile does not diminish higher confidence in the model's ability to simulate wave runup and replicate wave runup conditions recorded by a pressure transducer during low- and high-energy storm conditions. The sensitivity of modelled high-water wave runup conditions to the averaging period of the initial X-band radar-derived intertidal morphology and processing techniques, compared to a baseline DEM from Edina Digimap, is explored. To the authors' knowledge, this is the first time that cross-shore profiles have been extracted from an X-band radar-derived intertidal morphology to be used as input for a process-based model.

Variability in the resolution and coverage of the DEMs meant that idealised slope was used to represent the change in beach elevation in the inter-tidal zone captured by the radar. Modelled wave runup shows sensitivity to input DEM X-band derived topographies on some cross-shore profiles when applied in XBeach. Modelled high water wave runup on easterly cross-shore profiles showed greatest sensitivity to X-band derived DEMs processed using modelled, local water level outputs from the Met Office North West European Shelf seas model. This generated up to 0.25 m higher wave runup than the Camber Sands DEM from Edina Digimap LiDAR data, which could be important for overwashing and contribute to inundation (Lyddon *et al.*, 2020). Conversely, the Camber Sands DEM derived from composite LiDAR up to 2017 could be underestimating wave runup. This justifies the need for regular updates in intertidal morphology beyond the low water mark, further offshore than locally-organised beach profiling captures, to accurately represent beach slope for estimations of wave runup. XBeach has been shown to be more sensitive to beach slope as an input parameter, and increasing beach slope can also generate greater sensitivity to wave dissipation and turbulence (Wallbridge *et al.*, 2019). Modelled high water wave runup showed greatest sensitivity on profile 4, therefore XBeach was re-run using an X-Band derived DEM processed using observed, regional water level from the Dover tide gauge. This generated a shallower slope DEM as the Dover tide gauge records lower high-water levels than the Met Office North West European Shelf seas model simulates locally at Camber Sands, and subsequently lower high water wave runup in line with levels recorded by the Camber Sands DEM.

Regional vs local water level time series used to process X-band radar-derived intertidal morphology

It is evident that the water level time series used to generate DEMs from X-band radar outputs is a critical component of how these tools are used to capture coastal behaviours in process-based models. A local, modelled water level output or a regional, observed water level recorded by a tide gauge can be used to process the X-band derived DEM. Temporary local water level measurements, such as those provided by a tide gauge or an AWAC, would provide additional data to calibrate a model tide or apply harmonic analysis to predict the local tide for periods when the X-band radar is deployed. This would provide a local record of total water level at the study site, with accurate tidal range, to generate a high-resolution radar-derived DEM, for more accurate estimations of wave runup. This local X-band radar-derived DEM could be used to simulate day to day changes, with the model forced by the local tide gauge recorded water level.

The results presented here show the application of standard marine navigation X-band radars for deriving bathymetry and estimations of wave runup where there is no local control from a tide gauge. Without a local tide gauge control, the results presented here shows that a regional water level time series from a tide gauge provides good estimates of modelled wave runup hazards and along-shore variations in the hazard. The X-band radar-derived intertidal morphology processed from regional, observed water level at Dover tide gauge generates a shallower average beach slope compared with the X-band radar-derived DEM processed from the Met Office North West European Shelf seas modelled water level outputs, attributed to the difference in the tidal range shown in the tide gauge data and regional mode data.

If a user does not have a local or regional tide gauge control, then North West European Shelf seas model (or other equivalent models) outputs can be used effectively to generate a reduced resolution, highly variable DEM which can be processed to generate an idealised slope from which to calculate wave runup. These modelled wave runups on idealised slope X-band derived DEM from North West European Shelf seas model can still be used with confidence as there is good agreement within a similar range when compared against CS_DEM idealised slope and cross-shore variability. It would be valuable to validate these modelled wave runups from an X-band radar-derived DEM processed from the North West European Shelf seas modelled water level outputs against instrumental data to check wave runup at the time of high water. From a user's perspective, the X-band radar-derived DEM processed from the North West European Shelf seas model water level outputs is poorly constrained and a poorer resolution, but the modelled wave runup outputs are not substantially different from a higher resolution DEM, and so sufficient to capture overall local morphology and provide an acceptable assessment of overall beach slope change to characterise local wave runup.

It is assumed here that the cross-shore profiles from the X-band radar-derived DEMs processed from the regional observed water level at Dover tide gauge are more accurate because they are higher resolution. Comparison between the Dover tide gauge and Camber Sands North West European Shelf seas model outputs shows that the tide gauge doesn't capture the high and low water at Camber Sands well. The tide gauge overestimates low water, and underestimates high water compared to the local model outputs. Therefore the X-band radar-derived DEM processed from regional, observed water level at Dover tide gauge is bound to be shallower. This is turn generate smaller wave runup, like those generated by the CS_DEM and idealised slope derived from LiDAR. There is good agreement in water level records between Met Office North West European Shelf seas model outputs at Dover and the regional tide gauge at Dover, indicating that both should be used with a high level of confidence. Further work is needed to assess how best to use the North West European Shelf seas model outputs to derive accurate, higher resolution DEMs as this should represent a good alternative when a local tide gauge control is not available.

Averaging windows

The variability of idealised slope and subsequent sensitivity of modelled high-water wave runup conditions to the averaging period of the initial X-band radar-derived DEM was also explored. There is no substantial difference in elevation or idealised slope between the DEMs for each averaging period. There is a greater level of coverage and resolution in the DEMs with a longer averaging period. A 10-day averaging period is best if a radar is deployed and continuously collecting data for a number of months, and the researcher is interested in capturing small-scale features and bedforms in the inter-tidal zone and understanding shoreline evolution over a longer period. This requires additional computational power but will provide higher resolution DEMs to analyse and characterise temporal shoreline changes, or feed into a process-based model. A 1-day averaging period would be sufficient for capturing overall beach slope if a radar can only be deployed intermittently, or for short periods of time. A 1-day averaged DEM would enable a general assessment of overall beach slope change to capture storm response or for hazard assessments to see if there is a change in flood hazard or potential barrier breach risk. The best averaging period to use when post-processing X-band radar images depends on how long the radar was collecting data for and the aims of the research. Investment is needed in processing outputs from the radar to generate and ensure accurate results. Calibration and validation of the X-band radar DEMs via ground trothing, e.g. beach surveys, fixed cameras, drones, at the same time the marine radar is deployed is important to ensure confidence in the outputs (Parsons *et al.*, 2016). Further to this, there is a need for accurate, local water level, either modelled or monitored e.g. a 1-year AWAC deployment can be used to create a set of harmonics for tidal predictions. A longer averaging period provides improved resolution and coverage in the DEM, but it is at the discretion of the user to select the exact processing method and averaging period dependent on the aims of the research.

Application of X-band radars for deriving bathymetries and characterising coastal behaviours

X-band radars operate automatically and collect temporally- and spatially-continuous data over a wide area, in most weather conditions. Once best practices are identified for processing radar images based on the availability of a local water level time series and how the aims of the research determines averaging period, then X-band radar can be valuable for characterising coastal behaviours.

Standalone technique

The application of X-band radars for deriving bathymetries can be used as a standalone technique at a range of temporal scales for surveillance and monitoring of morphological change. The morphological response of intertidal areas to storm events is assessed using radar-derived DEMs collected to the east of Hilbre Island in the Dee Estuary (Bird *et al.*, 2017). Pre- and post-storm assessments were completed around 29 October 2006 to assess erosion and sediment loss from bedforms during the storm event, and the X-band radar-derived DEMs identified overall reduction of beach elevation and residual elevation change between pre- and post-storm surveys. This highlights the ability of X-band radar-derived DEMs to capture high frequency temporal changes, particularly on high energy coastlines comprised of mobile sediments. X-band radars have also been used to derive bathymetric-topographic change to inform engineering design at sites of critical infrastructure. The technique has been used to better understand shoreline change over three years at a proposed new nuclear power station at Sizewell, UK, and results illustrate baseline geomorphic behaviours in the intertidal zone that were previously unobserved by 20 years beach profiling, including bar interactions with outfall pipes and appearance of scour pits during high energy events (Wallbridge *et al.*, 2019). X-band radar-derived bathymetries can identify high frequency temporal

morphological changes, on a storm event timescale, or underlying trends in accretion and erosion which annual beach surveys may miss (Parsons *et al.*, 2016). Longer periods of deployment are required to identify inter- and intra-annual changes in beach morphology but are a cheaper option compared to LiDAR surveys or regular in-situ surveys.

Support other techniques

The application of X-band radars for deriving bathymetries can also be used to support other techniques. It can be used in combination with other observation data (e.g. autonomous surface, underwater, or airborne vehicles) which cannot be used continuously, and survey data to fill areas of missing data. This removes reliance on interpolation or filling in the gaps of cross-shore surveys. As shown here, cross-shore profiles can be extracted from the X-band radar-derived DEMs and applied in a process-based model to simulate morphological change and wave runup. Deployment of pressure transducers and collection of beach morphology surveys would be valuable to collect at the same time as the deployment of the X-band radar, to provide validation data. Ground-truthed radar-derived bathymetries could replace the reliance of local authorities or national bodies on beach profiles, which are time-consuming, and sometimes irregular, to inform shoreline management plans and long-term monitoring schemes.

6. Conclusion

High energy storm events pose a significant hazard at the coastal zone, and a serious problem by threatening ecological integrity, infrastructure, homes and even lives. Erosion and flood hazard management relies on understanding ongoing coastal processes, including the response of the coastal zone to previous storm events, to characterise and resolve local behaviours under present and future climate conditions. Storm events can alter the local wave climate at the coast by increasing significant wave height, which in turn poses an erosion hazard and can increase wave runup to potentially cause overwash and inundation. Standard marine navigation radar, operating at an X-band frequency, can be used to monitor local wave conditions and changes in intertidal morphology and foreshore slope. Outputs from an X-band radar can be used in standalone to generate Digital Elevation Models of the shoreline or use these outputs to in a process-based mode as an input depth file to simulate wave and erosion hazards.

This research applies a series of intertidal bathymetries derived from a standard marine radar deployed at Camber Sands, southeast England in XBeach, a process-based, storm response model, to assess wave runup hazard at the coast during a high energy storm event from the deployment period. Wave runup is sensitive to nearshore morphological variability and is used here as an indicator to demonstrate influence of a series of X-band radar-derived intertidal morphologies on local coastal behaviour. Nearshore variability is represented in a series of six X-band radar-derived intertidal bathymetries, processed using either i) local water level time series from the Met Office North West European Shelf seas model or ii) regional water level time series from the NTSLF Dover tide gauge in the temporal waterline algorithm. Intertidal bathymetries are also processed and averaged using i) 1; ii) 5; or iii) 10 days of radar outputs in the run up to a storm event with the highest significant wave height during the radar deployment, 18 June 2019.

Modelled wave runup shows up to 0.25 m sensitivity to input intertidal bathymetries. The slope and resolution of the radar-derived intertidal bathymetries is sensitive to the water level time series used, and coverage of the X-band radar-derived intertidal bathymetry improves with a longer averaging period. The results confirm that a local water level time series record from a local tide gauge is required alongside the X-band radar deployment to be used in the temporal waterline

algorithm to generate an accurate intertidal bathymetry. Locally measured water level would also be crucial for generating an accurate intertidal bathymetry for modelling two-dimensional morphological change. If the X-band radar-derived intertidal bathymetries are to be used just to obtain a general assessment of overall beach slope, general morphological change and what that might mean for wave runup hazard then a local tide gauge is not required. As shown here, model outputs from the regional Met Office North West European Shelf seas model or a regional tide gauge would be suitable and can be used in the temporal waterline algorithm to identify beach slope in intertidal bathymetries and model hydrodynamics, including wave runups, across a one-dimensional horizontal slope. An averaging period of 1 day could be used to obtain a general beach slope, but the coverage and resolution of the intertidal bathymetry is improved when a 10-day period is used. The processing technique to generate a X-band radar-derived intertidal bathymetry depends on the aim of the research. A local tide gauge control would be most important in the temporal waterline algorithm if the X-band radar-derived intertidal bathymetry is to be used for 2D morphological modelling, whereas outputs from a regional model or tide gauge could support hydrodynamic modelling. Ideally, a local tide gauge control would also be complimented by beach surveys, X-band radar deployment and process-based, numerical model runs to fully capture local coastal behaviours. This research highlights that X-band radar-derived intertidal bathymetries can be successfully applied in process-based numerical models to characterise local coastal behaviours and hazards, and processing techniques should be chosen based on the aims of the research.

References

Atkinson, J., Esteves, L.S., Williams, J.W., McCann, D.L. and Bell, P.S. 2018. The Application of X-Band Radar for Characterization of Nearshore Dynamics on a Mixed Sand and Gravel Beach. *Journal of Coastal Research*, (85 (10085)), pp.281–285. [Online]. Available from: https://doi.org/10.2112/SI85-057.1.

Barnard, P.L., van Ormondt, M., Erikson, L.H., Eshleman, J., Hapke, C., Ruggiero, P., Adams, P.N. and Foxgrover, A.C. 2014. Development of the Coastal Storm Modeling System (CoSMoS) for predicting the impact of storms on high-energy, active-margin coasts. *Natural Hazards*, 74 (2), pp.1095–1125. [Online]. Available from: https://doi.org/10.1007/s11069-014-1236-y.

Bell, P.S., Bird, C.O. and Plater, A.J. 2016. A temporal waterline approach to mapping intertidal areas using X-band marine radar. *Coastal Engineering*, 107, pp.84–101. [Online]. Available from: https://www.sciencedirect.com/science/article/pii/S037838391500157X.

Biausque, M. and Senechal, N. 2018. Storms impacts on a sandy beach including seasonal recovery: alongshore variability and management influences. *Revue Paralia*, 11, p.n02.1-n02.16.

Billson, O., Russell, P. and Davidson, M. 2019. Storm Waves at the Shoreline: When and Where Are Infragravity Waves Important? *Journal of Marine Science and Engineering*, 7 (5). [Online]. Available from: https://www.mdpi.com/2077-1312/7/5/139.

Bird, C.O., Bell, P.S. and Plater, A.J. 2017. Application of marine radar to monitoring seasonal and event-based changes in intertidal morphology. *Geomorphology*, 285, pp.1–15. [Online]. Available from: https://www.sciencedirect.com/science/article/pii/S0169555X16306493.

Bradbury, A., McFarland, S., Horne, J. and Eastick, C. 2003. DEVELOPMENT OF A STRATEGIC COASTAL MONITORING PROGRAMME FOR SOUTHEAST ENGLAND. In: *Coastal Engineering 2002*. WORLD SCIENTIFIC.pp.3234–3246. [Online]. Available from: https://doi.org/10.1142/9789812791306_0269.

Burningham, H. and French, J. 2017. Understanding coastal change using shoreline trend analysis supported by cluster-based segmentation. *Geomorphology*, 282, pp.131–149. [Online]. Available from: https://www.sciencedirect.com/science/article/pii/S0169555X16309503.

Burvingt, O., Masselink, G., Russell, P. and Scott, T. 2017. Classification of beach response to extreme storms. *Geomorphology*, 295, pp.722–737. [Online]. Available from: https://www.sciencedirect.com/science/article/pii/S0169555X17302970.

Channel Coastal Observatory. 2020. *Channel Coastal Observatory Data Viewer*. https://www.channelcoast.org/cco/.

Ciavola, P., Ferreira, O., Dongeren, A. van, Vries, J.V.T. de, Armaroli, C. and Harley, M. 2014. Prediction of Storm Impacts on Beach and Dune Systems. In: *Hydrometeorological Hazards*. John Wiley & Sons, Ltd.pp.227–252. [Online]. Available from: https://onlinelibrary.wiley.com/doi/abs/10.1002/9781118629567.ch3d.

Cohn, N. and Ruggiero, P. 2016. The influence of seasonal to interannual nearshore profile variability on extreme water levels: Modeling wave runup on dissipative beaches. *Coastal Engineering*, 115, pp.79–92. [Online]. Available from: https://www.sciencedirect.com/science/article/pii/S0378383916000168.

Cowell, P.J. and Thom, B.G. 1994. Morphodynamics of coastal evolution. In: R.W.G. Carter and C.D. Woodroffe, eds. *Coastal evolution, late quaternary shoreline morphodynamics.* Cambridge: Cambridge University Press.

Davidson, M.A., Aarninkhof, S.G.J., van Koningsveld, M. and Holman, R.A. 2006. Developing Coastal Video Monitoring Systems in Support of Coastal Zone Management. *Journal of Coastal Research*, pp.49–56. [Online]. Coastal Education & Research Foundation, Inc. Available from: http://www.jstor.org/stable/25741533.

Didier, D., Caulet, C., Bandet, M., Bernatchez, P., Dumont, D., Augereau, E., Floc'h, F. and Delacourt, C. 2020. Wave runup parameterization for sandy, gravel and platform beaches in a fetch-limited, large estuarine system. *Continental Shelf Research*, 192, p.104024. [Online]. Available from: https://www.sciencedirect.com/science/article/pii/S0278434319304078.

Environment Agency. 2014. *Broomhill Sands coastal defence scheme*. https://www.gov.uk/government/publications/broomhill-sands-coastal-defence-scheme/.

Ferreira, Ó., Plomaritis, T.A. and Costas, S. 2017. Process-based indicators to assess storm induced coastal hazards. *Earth-Science Reviews*, 173, pp.159–167. [Online]. Available from: https://www.sciencedirect.com/science/article/pii/S0012825217303161.

Guisado-Pintado, E. and Jackson, D.W.T. 2020. Monitoring Cross-shore Intertidal Beach Dynamics using Oblique Time-lapse Photography. *Journal of Coastal Research*, 95 (SI), pp.1106–1110. [Online]. Available from: https://doi.org/10.2112/SI95-215.1.

Hobbs, P., Gibson, A., Jones, L., Pennington, C., Jenkins, G., Pearson, S. and Freeborough, K. 2010. Monitoring coastal change using terrestrial LiDAR. *Geological Society of London Special Publications*, 345, pp.117–127.

Kerguillec, R., Audère, M., Baltzer, A., Debaine, F., Fattal, P., Juigner, M., Launeau, P., le Mauff, B., Luquet, F., Maanan, M., Pouzet, P., Robin, M. and Rollo, N. 2019. Monitoring and management of coastal hazards: Creation of a regional observatory of coastal erosion and storm surges in the pays

de la Loire region (Atlantic coast, France). *Ocean & Coastal Management*, 181, p.104904. [Online]. Available from: https://www.sciencedirect.com/science/article/pii/S096456911930078X.

Klemas, V. 2011. Beach Profiling and LIDAR Bathymetry: An Overview with Case Studies. *Journal of Coastal Research*, 27, pp.1019–1028.

Lyddon, C.E., Brown, J.M., Leonardi, N. and Plater, A.J. 2020. Sensitivity of Flood Hazard and Damage to Modelling Approaches. *Journal of Marine Science and Engineering*, 8 (9). [Online]. Available from: https://www.mdpi.com/2077-1312/8/9/724.

Mason, T., Bradbury, A., Poate, T. and Newman, R. 2009. NEARSHORE WAVE CLIMATE OF THE ENGLISH CHANNEL ? EVIDENCE FOR BI-MODAL SEAS. In: *Coastal Engineering 2008*. World Scientific Publishing Company.pp.605–616. [Online]. Available from: https://doi.org/10.1142/9789814277426_0051.

McCall, R.T., Masselink, G., Poate, T.G., Roelvink, J.A. and Almeida, L.P. 2015. Modelling the morphodynamics of gravel beaches during storms with XBeach-G. *Coastal Engineering*, 103, pp.52–66. [Online]. Available from: https://www.sciencedirect.com/science/article/pii/S0378383915001052.

McCall, R.T., van Thiel de Vries, J.S.M., Plant, N.G., van Dongeren, A.R., Roelvink, J.A., Thompson, D.M. and Reniers, A.J.H.M. 2010. Two-dimensional time dependent hurricane overwash and erosion modeling at Santa Rosa Island. *Coastal Engineering*, 57 (7), pp.668–683. [Online]. Available from: https://www.sciencedirect.com/science/article/pii/S037838391000027X.

Nuyts, S., Murphy, J., Li, Z. and Hickey, K. 2020. A Methodology to Assess the Morphological Change of a Multilevel Beach Cusp System and their Hydrodynamics: Case Study of Long Strand, Ireland. *Journal of Coastal Research*, 95 (SI), pp.593–598. [Online]. Available from: https://doi.org/10.2112/SI95-116.1.

Oh, J.-E., Chang, Y.S., Jeong, W.M., Kim, K.H. and Ryu, K.H. 2020. Estimation of Longshore Sediment Transport Using Video Monitoring Shoreline Data. *Journal of Marine Science and Engineering*, 8 (8). [Online]. Available from: https://www.mdpi.com/2077-1312/8/8/572.

Palmer, T., Nicholls, R.J., Wells, N.C., Saulter, A. and Mason, T. 2014. Identification of 'energetic' swell waves in a tidal strait. *Continental Shelf Research*, 88, pp.203–215. [Online]. Available from: https://www.sciencedirect.com/science/article/pii/S0278434314002660.

Parsons, A., Fish, P. and Siddle, R. 2016. Lessons from Strategic Coastal Monitoring. In: *Coastal Management*, Conference Proceedings. ICE Publishing.pp.251–262. [Online]. Available from: https://doi.org/10.1680/cm.61149.251.

Phillips, B.T., Brown, J.M., Bidlot, J.-R. and Plater, A.J. 2017. Role of Beach Morphology in Wave Overtopping Hazard Assessment. *Journal of Marine Science and Engineering*, 5 (1). [Online]. Available from: https://www.mdpi.com/2077-1312/5/1/1.

Poate, T.G., McCall, R.T. and Masselink, G. 2016. A new parameterisation for runup on gravel beaches. *Coastal Engineering*, 117, pp.176–190. [Online]. Available from: https://www.sciencedirect.com/science/article/pii/S0378383916301697.

Pollard, J.A., Spencer, T. and Brooks, S.M. 2018. The interactive relationship between coastal erosion and flood risk. *Progress in Physical Geography: Earth and Environment*, 43 (4), pp.574–585. [Online]. SAGE Publications Ltd. Available from: https://doi.org/10.1177/0309133318794498.

Pye, K. and Smith, A.J. 1988. BEACH AND DUNE EROSION AND ACCRETION ON THE SEFTON COAST, NORTHWEST ENGLAND. *Journal of Coastal Research*, pp.33–36. [Online]. Coastal Education & Research Foundation, Inc. Available from: http://www.jstor.org/stable/40928724.

Roelvink, D., Reniers, A., van Dongeren, A., van Thiel de Vries, J., McCall, R. and Lescinski, J. 2009. Modelling storm impacts on beaches, dunes and barrier islands. *Coastal Engineering*, 56 (11), pp.1133–1152. [Online]. Available from: https://www.sciencedirect.com/science/article/pii/S0378383909001252.

Saulter, A., Bunney, C. and Li, J.-G. 2016. *Application of a refined grid global model for operational wave forecasting*.

Senechal, N., Coco, G., Bryan, K.R. and Holman, R.A. 2011. Wave runup during extreme storm conditions. *Journal of Geophysical Research: Oceans*, 116 (C7). [Online]. John Wiley & Sons, Ltd. Available from: https://doi.org/10.1029/2010JC006819.

Serafin, K.A., Ruggiero, P. and Stockdon, H.F. 2017. The relative contribution of waves, tides, and nontidal residuals to extreme total water levels on U.S. West Coast sandy beaches. *Geophysical Research Letters*, 44 (4), pp.1839–1847. [Online]. John Wiley & Sons, Ltd. Available from: https://doi.org/10.1002/2016GL071020.

Siddorn, J., Good, S., Harris, C., Lewis, H., Maksymczuk, J., Martin, M. and Saulter, A. 2015. Research priorities in support of ocean monitoring and forecasting at the Met Office. *Ocean Science Discussions*, 12, pp.2617–2653.

Splinter, K.D., Turner, I.L., Reinhardt, M. and Ruessink, G. 2017. Rapid adjustment of shoreline behavior to changing seasonality of storms: observations and modelling at an open-coast beach. *Earth Surface Processes and Landforms*, 42 (8), pp.1186–1194. [Online]. John Wiley & Sons, Ltd. Available from: https://doi.org/10.1002/esp.4088.

Stockdon, H.F., Holman, R.A., Howd, P.A. and Sallenger, A.H. 2006. Empirical parameterization of setup, swash, and runup. *Coastal Engineering*, 53 (7), pp.573–588. [Online]. Available from: https://www.sciencedirect.com/science/article/pii/S0378383906000044.

Stockdon, H.F., Thompson, D.M., Plant, N.G. and Long, J.W. 2014. Evaluation of wave runup predictions from numerical and parametric models. *Coastal Engineering*, 92, pp.1–11. [Online]. Available from: https://www.sciencedirect.com/science/article/pii/S0378383914001239.

SurgeWatch. 2020. *A Database of UK Coastal Flood Events*. https://www.surgewatch.org/.

Turner, I.L., Harley, M.D., Short, A.D., Simmons, J.A., Bracs, M.A., Phillips, M.S. and Splinter, K.D. 2016. A multi-decade dataset of monthly beach profile surveys and inshore wave forcing at Narrabeen, Australia. *Scientific data*, 3, p.160024. [Online]. Nature Publishing Group. Available from: https://pubmed.ncbi.nlm.nih.gov/27070299.

Vousdoukas, M.I., Almeida, L.P. and Ferreira, Ó. 2011. Modelling storm-induced beach morphological change in a meso-tidal, reflective beach using XBeach. *Journal of Coastal Research*, pp.1916–1920. [Online]. Coastal Education & Research Foundation, Inc. Available from: http://www.jstor.org/stable/26482510.

Wallbridge, S., Dolphin, T. and Taylor, C.J.L. 2019. X-band radar as a tool for monitoring natural coastal behaviour and potential development impacts. *Journal of Operational Oceanography*, 12

(sup2), pp.S199–S211. [Online]. Taylor & Francis. Available from: https://doi.org/10.1080/1755876X.2018.1526462.

Williams, J.J., Esteves, L.S. and Rochford, L.A. 2015. Modelling storm responses on a high-energy coastline with XBeach. *Modeling Earth Systems and Environment*, 1 (1), p.3. [Online]. Available from: https://doi.org/10.1007/s40808-015-0003-8.

Willmott, C.J. 1981. ON THE VALIDATION OF MODELS. *Physical Geography*, 2 (2), pp.184–194. [Online]. Taylor & Francis. Available from: https://doi.org/10.1080/02723646.1981.10642213.

Willmott, C.J., Robeson, S.M. and Matsuura, K. 2012. A refined index of model performance. *International Journal of Climatology*, 32 (13), pp.2088–2094. [Online]. John Wiley & Sons, Ltd. Available from: https://doi.org/10.1002/joc.2419.

Appendix 1

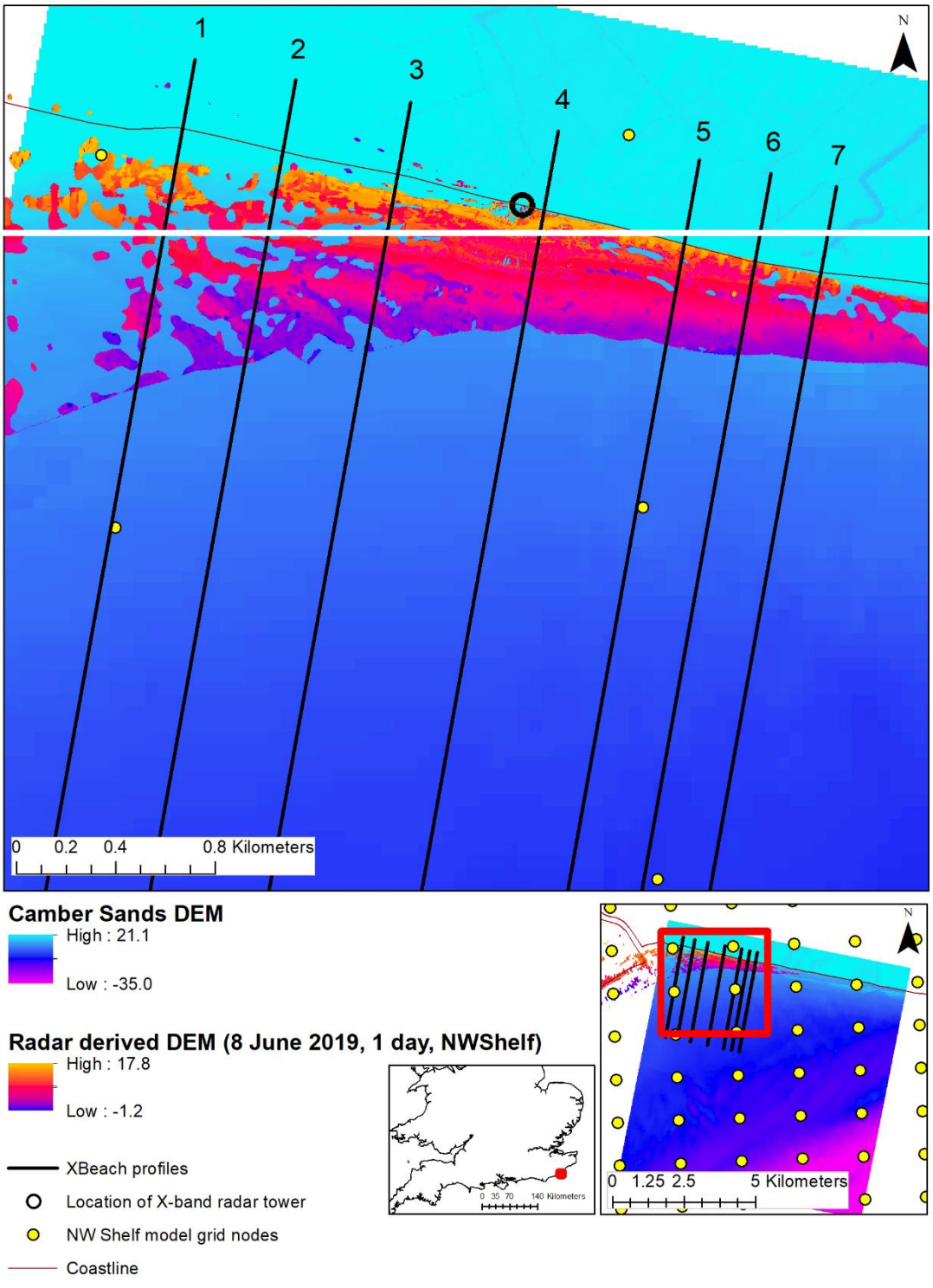
1
2
3
4
5
6
7
N
0 0.2 0.4 0.8 Kilometers
Camber Sands DEM
High : 21.1
Low : -35.0
Radar derived DEM (8 June 2019, 1 day, NWShelf)
High : 17.8
Low : -1.2
XBeach profiles
Location of X-band radar tower
NW Shelf model grid nodes
Coastline
0 35 70 140 Kilometers
N
0 1.25 2.5 5 Kilometers

Appendix 2

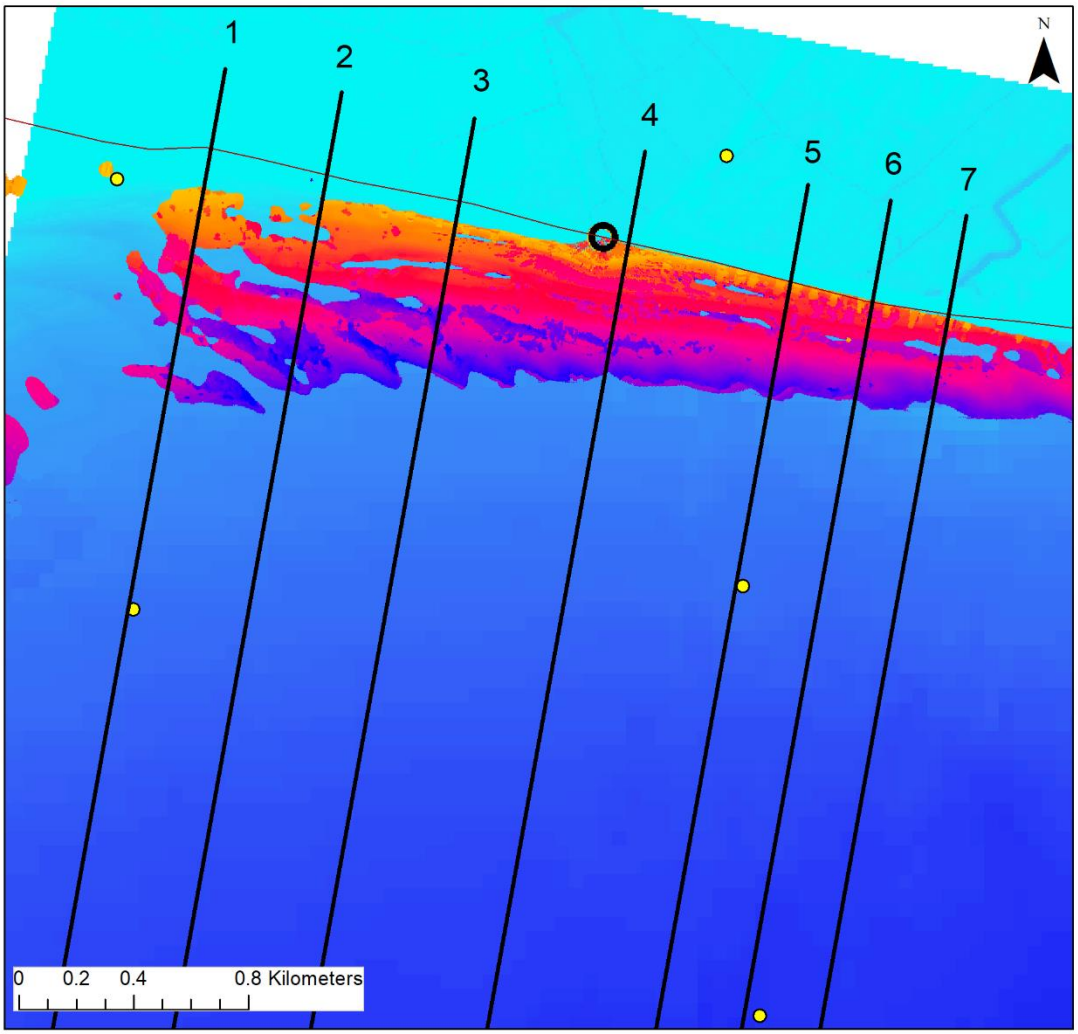

Camber Sands DEM

High : 21.1

Low : -35.0

Radar derived DEM (8 June 2019, 5 day, NWShelf)

High : 17.8

Low : -0.5

XBeach profiles

Location of X-band radar tower

NW Shelf model grid nodes

Coastline

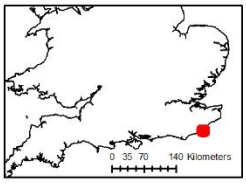

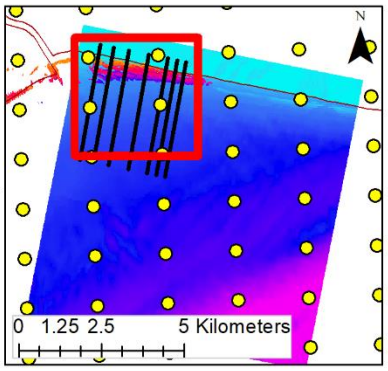

Appendix 3

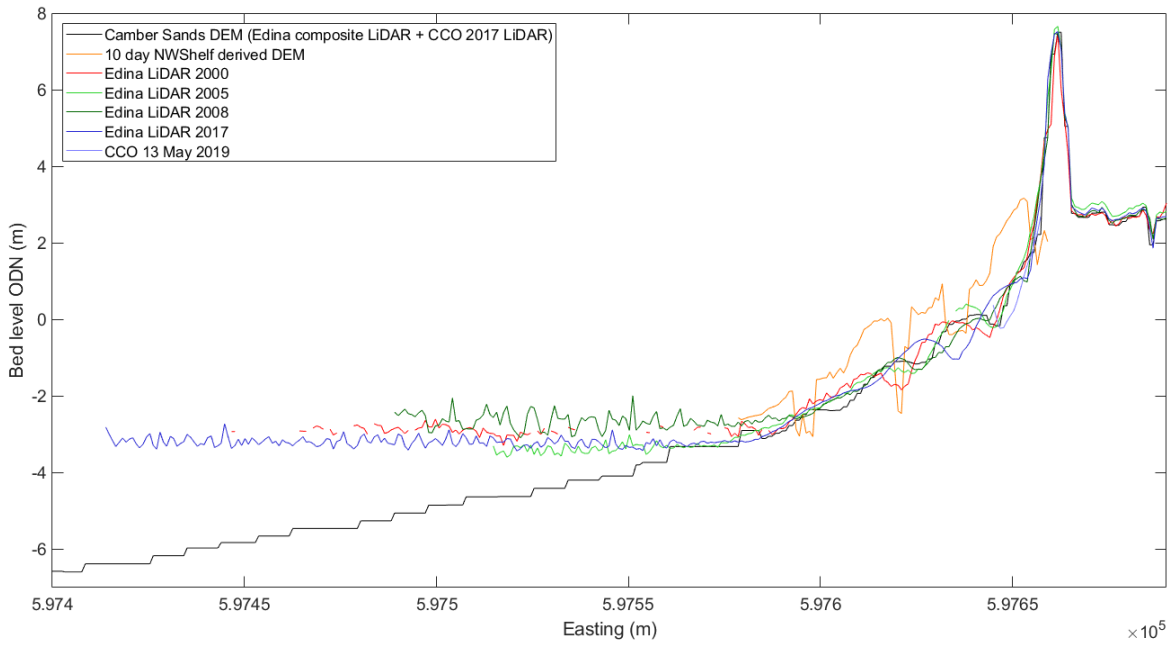

Appendix 3: A series of cross-shore beach profiles at Camber Sands on profile 3 taken from LiDAR surveys conducted between 2000 – 2020 and beach profile surveys from the Channel Coastal Observatory to demonstrate the variability in the profile from different data sources.